Jörg Peter Lichtenegger BSc

Structural and Biochemical Characterization of Different Monoglyceride Lipases

MASTER'S THESIS

to achieve the university degree of

Master of Science

Master's degree programme: Biochemistry and Molecular Biomedical Sciences

submitted to

Graz University of Technology

Supervisor

Assoc. Prof. Dr. Monika Oberer

Institute of Molecular Biosciences
Structural Biology

Graz, October 2015

AFFIDAVIT

I declare that I have authored this thesis independently, that I have not used other than the declared sources/resources, and that I have explicitly indicated all material which has been quoted either literally or by content from the sources used. The text document uploaded to TUGRAZonline is identical to the present master‘s thesis dissertation.

Date

Signature

„Parts of this work have been used for preparation of a manuscript (P. Aschauer, S. Rengachari, J. Lichtenegger, M. Schittmayer-Schantl,, K. M. P Das, N. Mayer, R. Breinbauer, R. Birner-Gruenberger,, C. C. Gruber, R. Zimmermann, K. Gruber, and M. Oberer: “Crystal structure of the *Saccharomyces cerevisiae* monoglyceride lipase YJU3p” which is currently in the submission phase.

Acknowledgements

I want to thank Dr. Monika Oberer for giving me the opportunity to do my master thesis in her group at the "structural biology floor" at the Institute of Molecular Sciences. I also want to thank her for all the scientific and personal advice she has been giving to me over the course of my work.

Furthermore I want to thank Philipp Aschauer who gave me guidance through my master thesis when I needed it and left me the freedom to do my own experiments when I wanted to test my theories.

I also want to thank all the rest of the "guys from the third floor" who not only gave me advice in scientific topics when needed but also kept up my mood when the work for my thesis seemed never-ending.

Last but not least I want to thank my whole family for supporting my decisions to stay in academia at every step. Most of all I want to thank my brother and my grandmother for their patience and help.

Abstract

Monoglyceride lipases (MGLs) are members of the serine hydrolase family and catalyse the cleaving of monoglycerides (MGs) into a free fatty acid and glycerol. They are ubiquitous in all kingdoms of life and take over different tasks in different organisms and different tissues. Their main task lies within energy homeostasis but they take over other important duties. In bacteria, for example, they are thought to take a role in detoxifying because short chained MGs are toxic to bacteria.

The goal of this work was to enhance the structural knowledge of different MGLs especially of YJU3p, the major MGL in yeast, and MGL from *Bacillus* sp. H257 (bMGL). Previous to this work, the three dimensional structure of a YJU3p solubility variant as un-complexed protein was available. The goal of my research was to obtain structures in complex with either inhibitors or substrate analogues. For bMGL, a un-complexed structure, and structures in complex with substrate analogues and inhibitors structures were known. To increase our knowledge of bMGL two specific variants have been expressed upon introducing mutations in the coding sequence. The resulting proteins were set up for crystallization.

In this thesis a structure for the YJU3p L175S 264R (s-YJU3p) solubility variant in complex with the substrate analogue C20 is described, with a focus on the structural changes in regard to the free form structure and the similarities and differences to the already known structure of bMGL in free form and in complex. Furthermore crystallization conditions for non-diffracting s-YJU3p crystals in complex with PMSF and the C18 substrate analogue are described. For bMGL two new variants, bMGL I145G and bMGL I145S, could be purified and crystallized but did not show well enough diffraction to collect datasets or solve the structures. The structure of bMGL I145G could be determined later in our lab (unpublished data, Krishna Mohan Padmanabha Das, Structural Biology, KFU-Graz), after the practical work for this thesis was finished and was also taken into account in the Discussion.

Zusammenfassung

Monglyceridlipasen gehören zur Gruppe der Serinhydrolasen. Sie katalysieren die Spaltung von Monoglyceriden in eine freie Fettsäure und ein Glyzerin. Monoglyceridlipasen sind ubiquitär in allen Organismen, wobei sie verschiedene Aufgaben, abhängig vom Gewebe und vom Organismus übernehmen. Hauptsächlich sind Monoglyceridlipasen im Energiestoffwechsel von Bedeutung. Sie übernehmen aber auch andere durchaus überlebenswichtige aufgeben. In Bakterien, für die vor allem kurzkettige Monoglyceride, toxisch sind, übernehmen sie eine wichtige „Entgiftungsaufgabe“.

Das Ziel dieser Arbeit war das Wissen über die dreidimensionalen Strukturen verschiedener MGLs, vor allem aber YJU3p, zu vertiefen. Bei YJU3p handelt es sich um die wichtigste MGL der Bäckerhefe *Saccharomyces cerevisiae*. Bereits vor Beginn dieser Arbeit war eine ungebundene Struktur einer YJU3p löslichkeits-Variante bekannt. Deshalb wurde der Fokus vor allem auf Komplexstrukturen, mit verschiedenen Inhibitoren und kovalent gebundenen Substratanalogen, gelegt. Das zweite Enzym von Interesse war die MGL aus dem *Bacillus* sp. H257 (bMGL). Für bMGL waren bereits Strukturen in freier Form, und in Komplex mit verschiedenen Inhibitoren und Substratanalogen bekannt. Um nun zusätzliche Informationen zu erhalten wurde versucht zwei Varianten, nämlich bMGL I145S und bMGL I145G zu reinigen und zu kristallisieren.

In dieser Arbeit wird nun eine neue Struktur der YJU3p löslichkeits-Variante in Komplex mit dem Substratanalog C20 vorgestellt und diskutiert. Der Fokus liegt hierbei auf den strukturellen Änderungen, die durch das kovalente gebundene Substratanalog auftreten, und auf den Ähnlichkeiten und Unterschieden zu den bereits vorhandenen Strukturen von bMGL. Für YJU3p L175S Q264R (s-YJU3p) in Komplex mit PMSF und dem Substratanalog C18 konnten außerdem Kristallisationsbedingungen beschrieben werden, welche allerdings nur nicht streuende Proteinkristalle hervorgebracht haben. Außerdem werden noch Kristallisationsbedingungen für zwei weitere bMGL Varianten (I145S, I145G) beschrieben, die zwar streuende Kristalle hervorgebracht haben, von denen aber

aufgrund zu geringer Streuung kein interpretierbarer Datensatz aufgenommen werden konnte. Die Struktur von bMGL I145G konnte nach dem Abschluss der praktischen Arbeit für diese Masterarbeit in unserem Labor (unpublished data, Krishna Mohan Padmanabha Das, Structural Biology, KFU-Graz) noch gelöst werden und wurde deshalb für die Diskussion ebenfalls herangezogen.

Table of Contents

1. Introduction 1
1.1. Lipases 1
1.2. Monoglyceride Lipases 1
1.3. Monoglycerides 2
1.4. Inhibitors and Substrate Analogues 3
1.5. Monoglyceride Lipase from *Bacillus* sp. H257 (bMGL) and Human (hMGL) 4
1.6. Monoglyceride Lipase from *Saccharomyces Cerevisiae* (YJU3p) 5
1.7. Crystallization 6
1.8. X-Ray Diffraction Analysis 8
2. Methods 11
2.1. Transformations of Expression Vectors into *E.coli* Strains 11
2.1.1. bMGL (I145S, I145G) 11
2.1.2. s-YJU3p 11
2.2. Protein Expression 11
2.2.1. bMGL (I145S, I145G) 11
2.2.2. s-YJU3p 12
2.3. Protein Purification 12
2.3.1. bMGL 13
2.3.2. s-YJU3p 13
2.4. s-YJU3p Activity Assay with the JZL 184 Inhibitor 14
2.5. Crystallization 14
2.5.1. bMGL I145S and bMGL I145G 15
2.5.2. s-YJU3p Inhibitor Complex 15
2.6. Structure Determination 17
2.6.1. X-Ray Diffraction 17

2.6.2. Data Processing and Refinement 17
3. Results 18
3.1. Purification 18
3.1.1. bMGL 18
3.1.2. s-YJU3p 20
3.2. YJU3p-JZL 184 Activity Assay 21
3.3. Crystallization and Data Collection 21
3.3.1. bMGL I145S and bMGL I145G 21
3.3.2. s-YJU3p 26
3.3.3. s-YJU3p Cocrystallization 28
4. Discussion 31
4.1. bMGL I145G 31
4.2. s-YJU3p 32
5. Collaborations 42
6. References 43
7. Supplemental 46
7.1. HSQC NMR 46
7.1. Protein and DNA sequences 47
7.1.1. YJU3 L175S Q264R DNA sequence 47
7.1.2. YJU3p WT and YJU3p L175S Q264R Protein Sequences 47
7.1.3. bMGL Wildtype and bMG LI145G Mutant Sequence Alignment 48
7.1.4. bMGL Wildtype and bMG LI145S Mutant Sequence Alignment 49
7.1.5. Multiple MGLs Sequence Alignments 50

1. Introduction

1.1. Lipases

Lipases are enzymes belonging to the family of serine hydrolases, they catalyze the hydrolysis of ester bonds in lipids, following the general reaction scheme in figure 1. They can be classified by their substrates (e.g. Tri-, Di-, Monoglyceride lipases, Figure 2).

Figure 1 General reaction scheme for hydrolases

1.2. Monoglyceride Lipases

Monoglyceride lipases (MGLs, EC 3.1.1.23) are enzymes that specifically catalyze the degradation of a monoglyceride (MG) into glycerol and a fatty acid (FA). In the process of intracellular lipolysis, stored triglycerides get successively degraded into

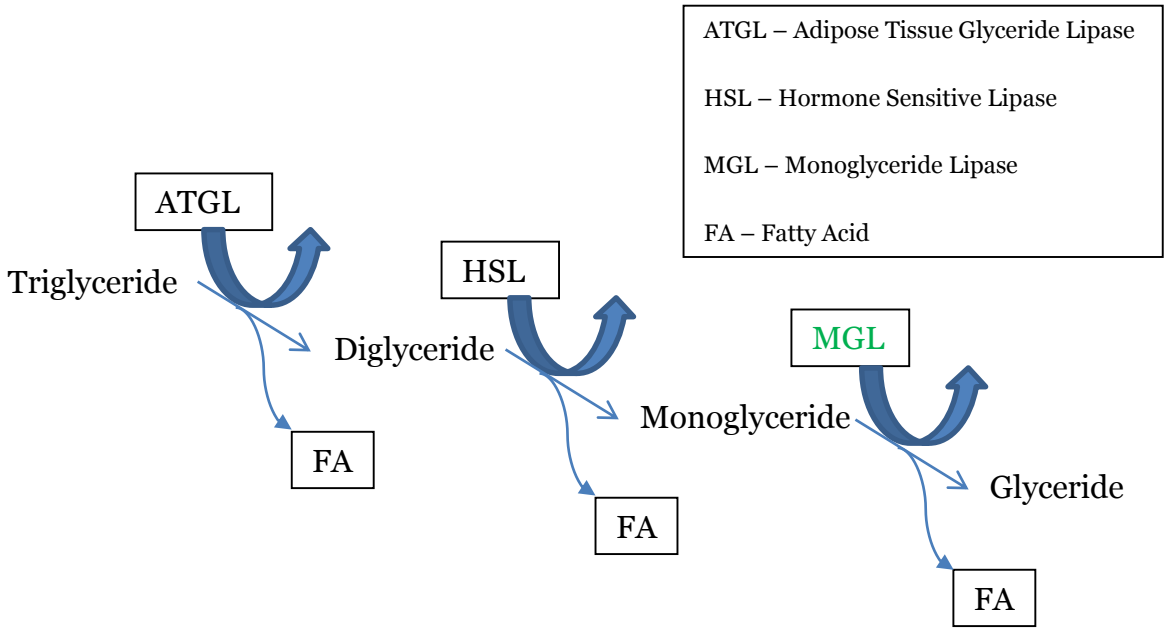

Figure 2 Schematic representation of the degradation of triglycerides into a fatty acid and glycerol. The last step is catalyzed by Monoglyceride Lipase (MGL).

diglycerides, monoglycerides and glycerol molecules (Figure 2, 3)(*7*). Adipose tissue glyceride lipase (ATGL) and hormone sensitive lipase (HSL) catalyze the first step and the second step of lipolysis (Figure 2) (*8-11*). MGLs carry out important, but different roles in all kingdoms of life starting from bacteria, where MGs are cytotoxic (*12-15*), to archaea to mammals where, MGLs participate in energy homeostasis and the endocannabinoid system, therefore regulating different essential processes like appetite and pain regulation (*7, 16-22*). Additionally MGLs have been identified to play a role in different kinds of cancer (e.g. melanoma, breast-, ovarian-, and colorectal

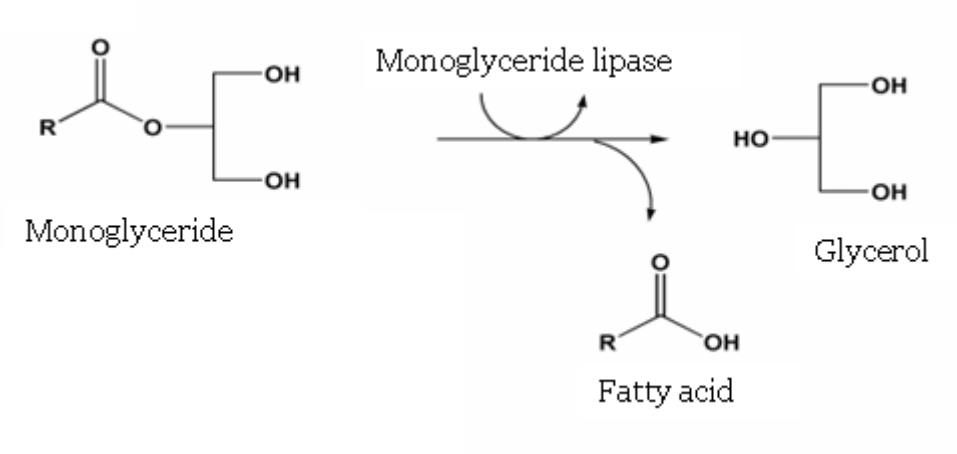

Figure 3 Schematic representation of the last step of lipolysis

cancer) (*23, 24*). Although a MGL in rat adipose tissue has already been described in 1976, structural information was only available in 2010 when the structure of human MGL (hMGL) could be determined(*7, 12, 19, 21*). In 2012 the structure of a bacterial MGL (bMGL from *Bacillus* sp. H254) could be solved and showed a striking overall structural similarity to hMGL with a sequence identity of only 17% (*1*).

1.3. Monoglycerides

Monoglycerides are short-lived intermediates in the lipid metabolism, which for example can be supplied intracellularly by the degradation of triglycerides (TGs) (Figure 2, 3), or from TGs that are taken up from food or secreted from the liver and degraded in the blood plasm by lipoprotein lipase (*25*).

The substrate specificity and the reaction rates of MGLs can be quite different from different organisms degrading different substrates (Figure 4) (*18, 26*).

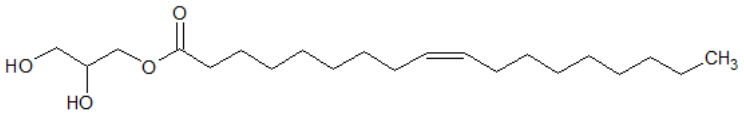

1-Oleoyl-*rac*-glycerol

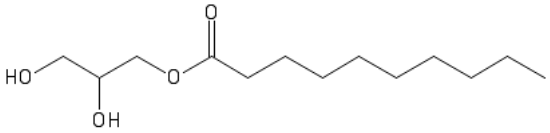

1-Decanoyl-rac-glycerol

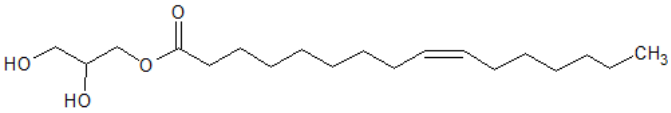

1-Monopalmitoleoyl-*rac*-glycerol

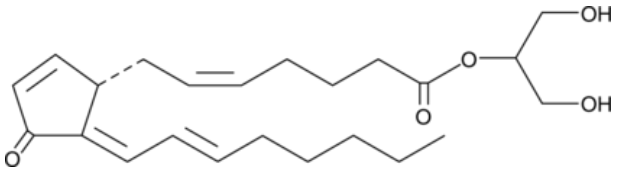

15-deoxy-Δ12, 14-prostaglandin J2-2-glycerol ester

Figure 4 Selection of natural substrates of MGLs

1.4. Inhibitors and Substrate Analogues

Different inhibitors and substrate analogues have been used for soaking and cocrystallization attempts (Figure 5). PMSF is known for inhibiting serine hydrolases and JZL 184 is a commercially available inhibitor for human MGL (hMGL) (*27, 28*). The substrate analogues ranging from C14 to C20 (C14, C16, C18 and C20) were provided to us by our cooperation partners from Medical University of Graz and Graz University of Technology (Chapter 5). In the substrate analogs, the phosphor and the oxygen atom act as 'substitutes' for carbon atoms in the MG substrates. Therefore, the substrate analog called C14 has actually a carbon chain consisting of only 12 carbon atoms as illustrated in Figure 5.

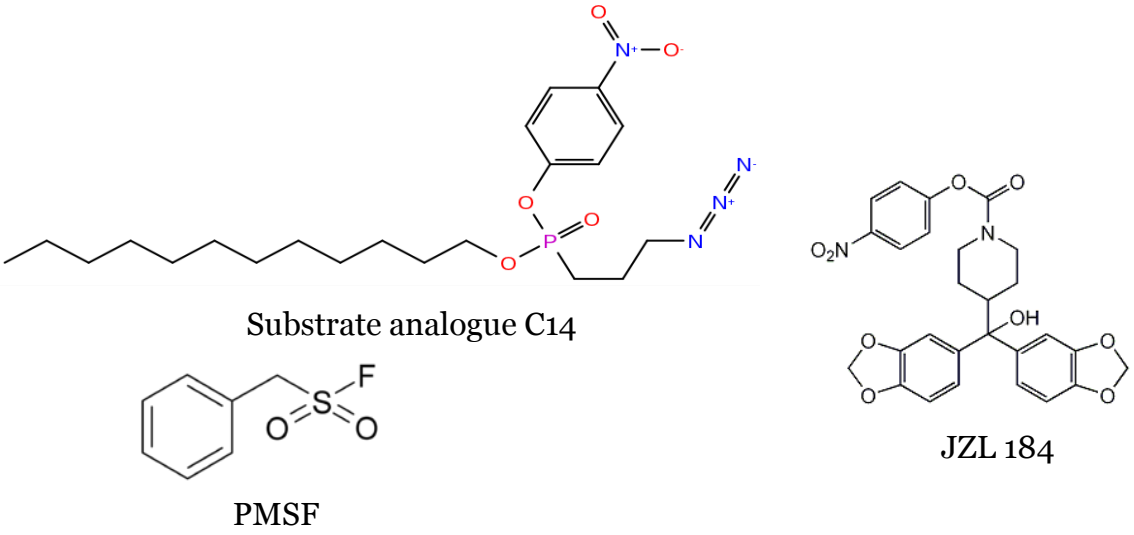

Figure 5 Substrate analogues and inhibitors used for soaking and co-crystallization attempts

1.5. Monoglyceride Lipase from *Bacillus* sp. H257 (bMGL) and Human (hMGL)

In 2012 MGL from the thermophile *Bacillus* sp. H257 was the second MGL structure to be solved after the human MGL (*1, 21*). bMGL is a 250 amino acid (28.7 kDa) enzyme, that shows high specificity for MGs with the highest specificity shown for 1-monolauroylglycerol (1-LG)(*26*). Although the overall sequence identity between these two orthologues is relatively low, with only 17% and an even lower identity in the cap

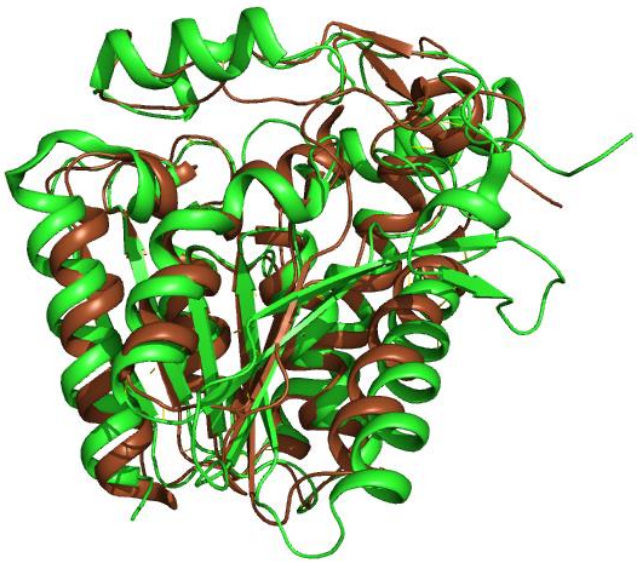

Figure 6 Superposition of free form bMGL (PDB 3RLI) and hMGL (PDB 3JW8) (RMSD 1.372Å)

region with only 10%, the overall structural conservation is strikingly high (RMSD 1.372Å, Figure 6). Both possess an α/β hydrolase fold, although in bMGL it is a minimal fold lacking the first β strand, and a flexible cap region (Figure 7). hMGL shows the highest substrate specificities for 1- decanoyl-rac-glycerol (1-DG) and 15-deoxy-Δ12,14-prostaglandin J2-2-glycerol ester (15d-PGJ2-G)(Figure 5)(*29, 30*). Extensive structural studies of bMGL and different variants in complex with either inhibitors or natural substrates showed plasticity in the cap region, with several different conformations being seen in the crystal structures (*31*). It was shown that the residue isoleucine 145 plays an important role in bMGL by acting as a gatekeeper through restricting the size of the binding pocket, therefore being an interesting target for structural studies (*31*). The residue 145 was mutated to glycine and to serine. Using monoglyceride hydrolase (MGH) assay, it could be shown that the flexibility but also the hydrophobicity of the residue is important for the activity of bMGL (*31*).

1.6. Monoglyceride Lipase from *Saccharomyces Cerevisiae* (YJU3p)

YJU3p is a 313 amino acid long protein that has been identified to be the functional orthologue of the mammalian MGL in the yeast *Saccharomyces cerevisiae*. It shares

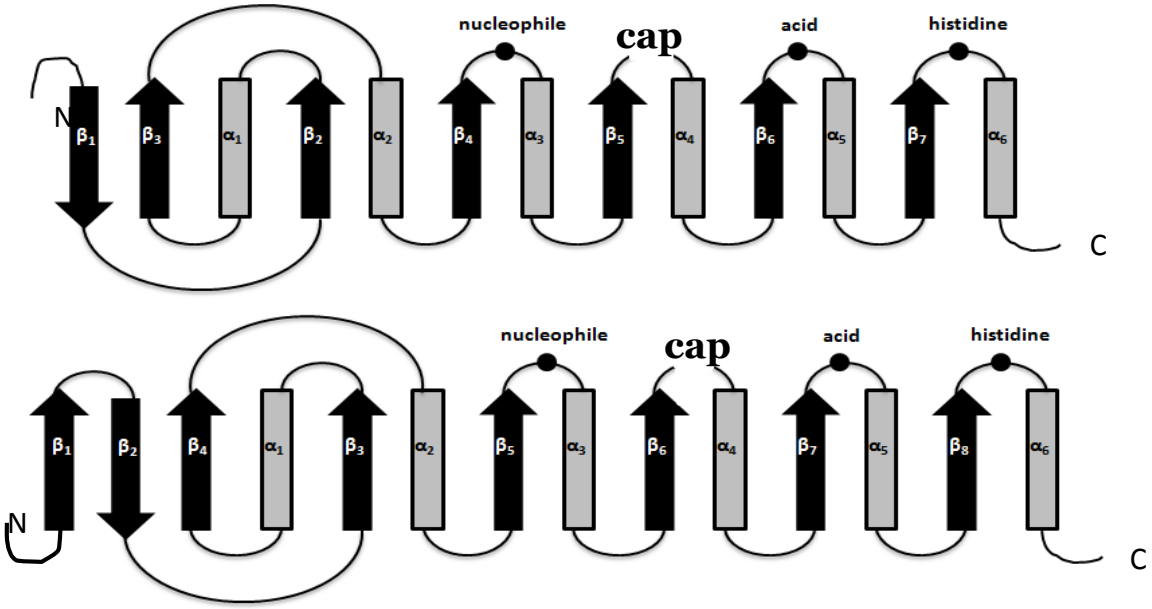

Figure 7 (A) Schematic representation of minimal α/β hydrolase fold observed in the structure of bMGL. (B) Schematic representation of canonical α/β hydrolase showing a backbone β strands and 6 α helices; N and C represent the respective termini of the protein. [Figure and text taken from (*1*)]

more than 20% of sequence identity with human MGL and is the major MGL *in yeast* accounting for 90% of the MGL activity (*32, 33*). The first structure of YJU3p L175S Q264R (s-YJU3p), a solubility variant, was determined in our group (unpublished, P. Aschauer) and showed remarkable structural similarities to the structures of bMGL and hMGL. It has the typical α/β hydrolase fold and a flexible cap region (Figure 7). In the free, un-complexed structure of the YJU3p solubility variant a partially open and a closed form could be observed in different chains. The catalytic triad could be identified unambiguously to comprise of His281, Asp251 and Ser123.

1.7. Crystallization

The major step in obtaining a protein structure from X-ray diffraction, is the crystallization of the protein. Growing a crystal suitable for X-ray structure determination is influenced by many different parameters in regard to the protein and the environment of the crystallization. The formation of a crystal nucleus and the growth of the crystal are heavily influenced by the concentration and homogeneity of the protein, the buffer system, the concentration and the types of salt and additives, the pH, temperature and the setup of the crystallization etc. There are dozens of parameters that influence protein crystallization. One important aspect is the crystallization setup, two of the most common set ups are hanging drop and sitting drop crystallization which are part of the vapor diffusion crystallization techniques. In hanging drop crystallization (Figure 8) the protein is typically mixed with precipitant

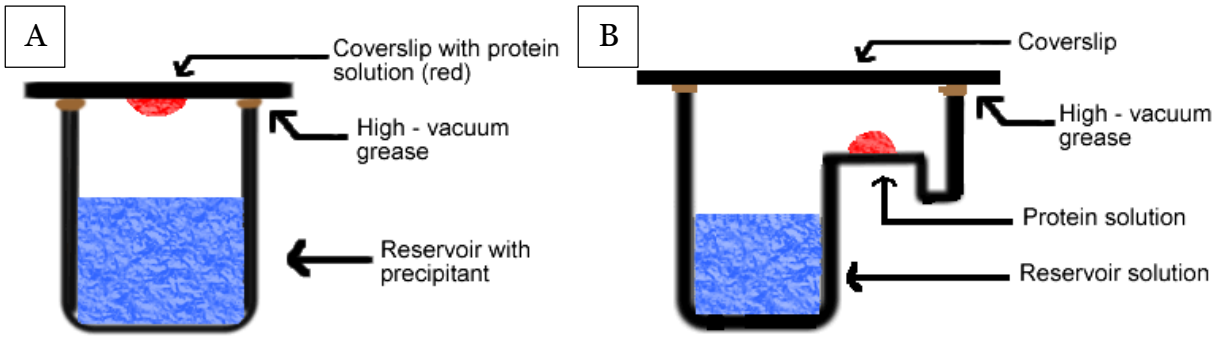

Figure 8 Scheme of the hanging drop method (A).Scheme of the sitting drop method (B) [Figure taken from (3)].

on a siliconized glass coverslip. The coverslip is placed on the reservoir in a manner that the drop is hanging over the precipitant solution. The chamber is sealed air tight with vacuum grease to prevent drying out of the mixture. Another common vapor

diffusion technique is sitting drop crystallization (Figure 8). In this case the drop sits on a pedestal next to the reservoir the crystallization plates used for this technique are usually closed with sealing tape. As shown in figure 9 and 10 the crystal growth is heavily dependent on protein concentration and solubility. The main point in vapor diffusion crystallization is to get the protein in your crystallization setup into a supersaturated state. This is accomplished by the higher concentration of precipitant in the reservoir solution leading to the diffusion of water from the crystallization drop into the reservoir solution and therefore an increase in protein concentration in the drop (Figure 10). As shown in figure 10, following the curve of the vapor diffusion crystallization, with rising concentration the protein shifts from the under-saturated zone through the metastable zone to the nucleation zone. This happens due to the diffusion of water molecules from the drop to the reservoir. In the nucleation zone the protein concentration in the solution is lowering when crystal nuclei are formed. This shifts the concentration back to the metastable zone where crystal growth occurs until enough of the protein goes into the crystalline solid state to shift the supernatant back into the under-saturated zone. With respect to crystallization reagents two common approaches are grid screens and sparse matrix screens. In grid screens only two variables are changed (e.g. precipitate concentration and pH). Sparse matrix screens use prior information regarding likelihood of crystallization from databases and contain statistically chosen crystallization conditions which proved successful for specific proteins (e.g. MembFac, Hampton Research or MemSys Molecular

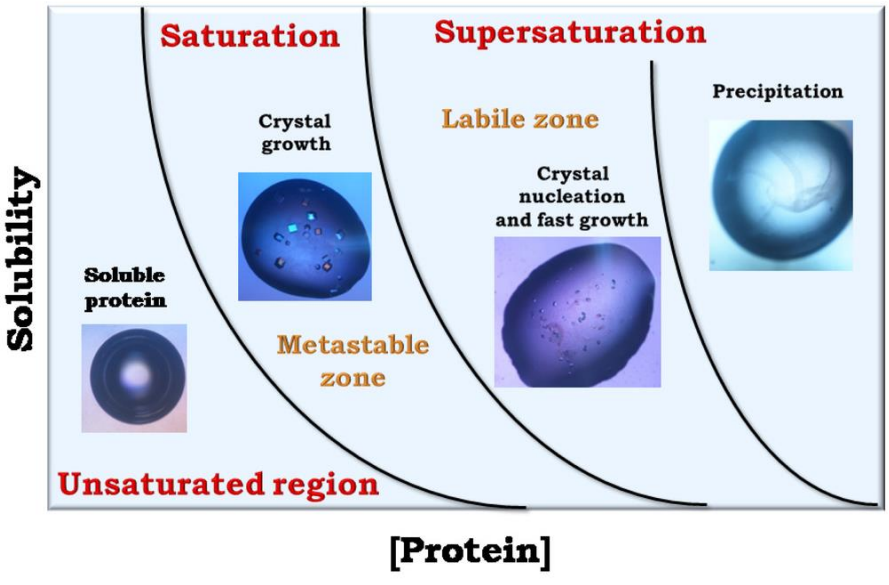

Figure 9 Schematic solubility curve for a protein, as a function of the protein concentration. [Figure taken from (6)]

Dimensions for membrane proteins) or for proteins in general (e.g. Morpheus Molecular Dimensions).

1.8. X-Ray Diffraction Analysis

There are two different methods used in generating X-rays for structure determination.

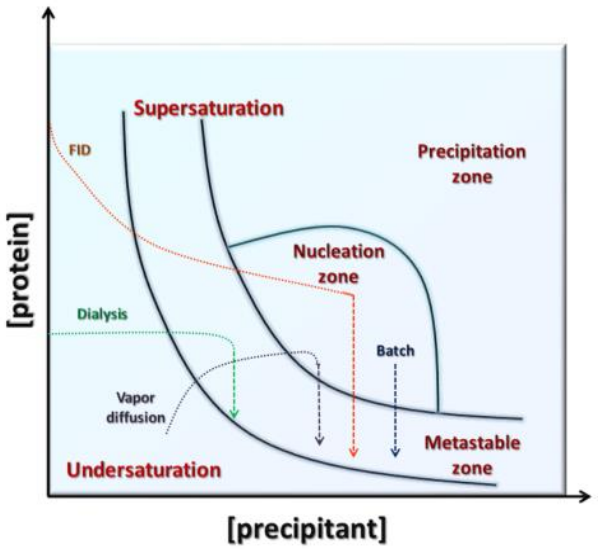

Figure 10 A simplified protein crystallization phase diagram. The different routes of reaching nucleation and metastable zones for the four main crystallization techniques are also shown. [Figure and text taken from (*6*)]

In rotating anodes or X-ray tubes a heavy metal (e.g. copper, molybdenum anode) is bombarded with electrons emitted by a heated cathode filament (e.g. tungsten) in vacuum. As the electron beam impacts the anode, two (*4, 5*) different kinds of X-ray radiation are produced. The so-called "Bremsstrahlung" has a continuous spectrum and is emitted when a charged particle (e.g. electron) gets accelerated/decelerated. The characteristic X-ray emission is emitted when an electron is knocked out of one of the inner shells and is replaced by an electron from a higher shell in the atoms of the anode material (Figure 11). The radiation emitted by this process is characteristic for the anode material and has a specific energy. Only the characteristic radiation is used for X-ray diffraction analysis. At synchrotron facilities X-rays are generated by electrons that are accelerated close to the speed of light and are bent by powerful magnetic devices in the so called storage ring. The production of synchrotron radiation is similar

to the Bremsstrahlung, namely that the electrons emit intensive radiation due to the acceleration in these devices. Accordingly, the radiation has a continuous spectrum and the synchrotron radiation is tuneable (Figure 12). Well-ordered protein crystals are diffracting X-rays in discrete patterns. Each such diffraction spot represents a wave with an amplitude and a phase. The distance between the spots in this diffraction pattern is only dependent on the unit cell dimensions. Once a crystal is obtained, it is exposed to X-ray diffraction to derive important information on the protein. On a first glance, protein crystallographers typically check the dimensions of the unit cell, especially whether the unit cell is big enough for the crystal to be made up of protein and the diffracting crystal is not made of salt (which would result in a much smaller unit cell). Systematic extinction can be present if the space group has a translational element. The structural information is contained in the intensities of the spots. However, the phase of the wave is unknown leading to the terminology of the crystallographic phase problem.

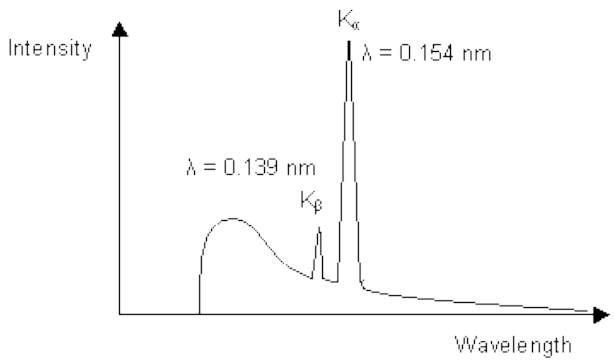

Figure 11 The diagram above illustrates the characteristic X-ray emission spectrum that is obtained from a copper target [Figure and text taken from (*4*)]

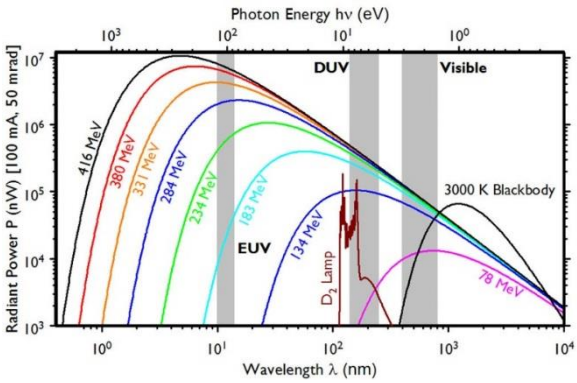

Figure 12 Synchrotron Radiation Spectrum emitted by the synchrotron ultraviolet radiation facility (SURF) at 416 MeV,380 MeV, 331 MeV, 284 MeV, 234 MeV, 183 MeV, 134 MeV, and 78 MeV in comparison to a 3000 K blackbody and a deuterium lamp. [Figure and text taken from (*5*)]

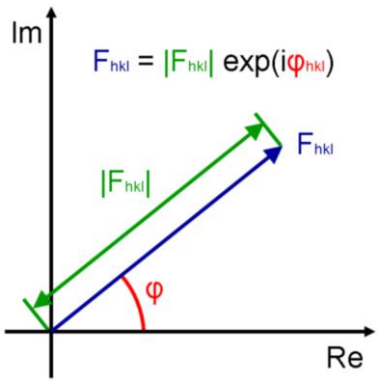

Figure 13 Argand diagram Representation of the phase problem |Fhkl| amplitude ϕ phase [Figure and text taken from (2)]

$$a) I(\vec{R}) = F(\vec{R})F^*(\vec{R}) = |F(\vec{R})|^2$$

As shown in formula a) and figure 13 the square root of the intensity (I_R) is the absolute value of the structure factor F_R. As shown in formula b) the knowledge of the phase is crucial for calculating the electron density ρ_R, therefore different approaches to solve the phase problem have been developed.

$$b) \rho(\vec{r}) = FT^{-1}(F(R)) = \iiint F(\vec{R})\, e^{-2\pi i \vec{r}\vec{R}}\, d^3\vec{R}$$

Whereas most methods for solving the phase problem like Multi-wavelength Anomalous Diffraction (MAD) and Multiple Isomorphous Replacement (MIR) need additional crystals, one approach that does not need them, after the initial dataset is obtained, is molecular replacement (MR). For MR an additional 3D structure that has a high enough structural similarity to the structure in question is needed. A model can be obtained by many different ways from theoretic calculations to homologues that have already been structural characterized. Since the structure of the protein in question still remains unknown at this point and can only be predicted, the search for a suitable model is one of the crucial steps for MR. After model selection, Patterson functions of the model and the data set are calculated. The outcome of the Patterson function are distances between atoms in the structure, so after the functions are calculated the model is rotated and translated until a good fit to the original data is accomplished. Afterwards the phase information can be calculated by using the atom coordinates of the model. Thus, the phases are calculated from the model, a wrong choice leads to uninterpretable density maps. Once a structure is obtained it gets refined, using programs like Refmac5 (*34*) and Coot (*35*). When the structure is

sufficiently refined it can be evaluated using a molecular visualization program like PyMOL (*36*). A crucial part of the structure determination is the evaluation and interpretation process.

2. Methods

2.1. Transformations of Expression Vectors into *E.coli* Strains

2.1.1. bMGL (I145S, I145G)

1µl of a pET28a(+) (Novagen, Merck, Whitehouse Station, USA) vector(100ng/µl) with the gene for the MGL from *Bacillus sp. H257* cloned between the NdeI and XhoI sites was incubated with 200 µl BL21 (DE3) *E.coli* cells on ice for 30 minutes (*37*). Afterwards the mixture was put into a water bath for a heat shock of 45 seconds at 42°C. The cells were again put on ice for two minutes and 800µl of Luria-Bertani broth were added. After growing the cells for 45min at 37°C, they were centrifuged at 3,3g (Centrifuge 5415R, Eppendorf AG, Hamburg Germany) for 1 minute. 800µl of the supernatant got discarded and the rest was plated on LB-Agar plate with kanamycin (40µg/ml) and incubated over night at 37°C.

2.1.2. s-YJU3p

1µL (100ng/µl) pPro Ex Htb vector (Invitrogen, Carlsbad, California, USA), cloned with the gene for s-YJU3p between the BamHI and EcoRI, was incubated with 200µL chemically competent BL21 (DE3) *E.coli* cells for 30min on ice (*37*). Afterwards it was heat shocked for 45 seconds in a water bath at 42°C and was then kept on ice for 2 minutes to recuperate. The cells were mixed with 800µL of Luria-Bertani broth and kept on 37°C for 45 minutes. Centrifuged for 1 minute (3,3g, Centrifuge 5415R, Eppendorf AG, Hamburg Germany) and 800µL of the supernatant were thrown away. The pellet was resuspended in the remaining supernatant and the suspension was plated on LB-agar plates with ampicillin (100µg/mL) and incubated overnight at 37°C.

2.2. Protein Expression

2.2.1. bMGL (I145S, I145G)

An *E.coli* BL21 (DE3) colony grown on an LB-Agar plate (Chapter.2.1.1) was inoculated into sterile LB broth (40µg/ml Kanamycin) for an overnight culture at 37°C and 180rpm. 10ml of the overnight culture were used to inoculate 500ml of sterile LB broth

(40µg/ml Kanamycin) for the main culture. The main culture was grown at 37°C and 180rpm until it reached an optical density (600nm) of 0.4 to 0.6, at this point the expression was started by adding 1M IPTG to a final concentration of 1mmol/l. After 4 hours of protein expression the cells were harvested by centrifuging for 10min at 2831g (Avanti J-26XP centrifuge, rotor JA 10, Beckman-Coulter GmbH, 47807 Krefeld, Germany).The supernatant was discarded and the pellets were stored at -20°C.

2.2.2. s-YJU3p

A single *E.coli* BL21 (DE3) colony with the gene for s-YJU3p obtained from an LB-Agar plate (Chapter.2.1.2) was inoculated into 150ml sterile LB broth (100µg/ml ampicillin) and incubated at 37°C and 180rpm overnight. 10ml of the overnight culture were inoculated into flasks containing 500ml sterile LB media (100µg/ml ampicillin). The cultures were grown at 37°C and 180rpm until they reached an optical density (600nm) between 0.4 and 0.6. Overexpression was induced by adding 1M IPTG to a final concentration of 1mmol/l. After expressing protein at 37°C and 180rpm for 4 hours, the cells where harvested by centrifuging for 10min at 2831g (Avanti J-26XP centrifuge, rotor JA10, Beckman-Coulter GmbH, 47807 Krefeld, Germany). The resulting pellet was divided into aliquots. Each aliquot was resuspended in 50ml 0.9%NaCl solution and centrifuged for 30 min with 3220g (Centrifuge 5180R, Eppendorf AG, Hamburg Germany). The supernatant was discarded and the pellets were stored at -20°C.

2.3.Protein Purification

All purifications were performed using self-packed Ni-NTA (QIAGEN GmbH, 40724 Hilden, Germany) columns. During the different steps of purification gel samples were collected to monitor the purification process and the purity of the protein, the samples for SDS gel electrophoresis were taken after lysis from the supernatant and the pellet, during the purification process, from the flow through, the washing and the elution fraction. For gel electrophoresis a Mini PROTEAN^{R} Tetra Cell (Bio-Rad Laboratories Ltd., Hemel Hempstead, UK) and an unstained protein marker (Fermentas GmbH, St. Leon-Rot, Germany) were used. The gels were stained with coomassie brilliant blue solution (0.5% coomassie R brilliant blue, 50% ethanol, 10% acetic acid) and destained in either destaining solution (30% Isopropanol, 10% Glacial Acetic Acid) or water overnight.

2.3.1. bMGL

bMGL I145S and bMGL I145G variants were purified under the same conditions with the same solutions.

Cell pellets (see Chapter 2.3.1) were thawed and resuspended in lysis buffer (Tris pH 7.5, 100mmol/l NaCl). The suspension was homogenized (ULTRA TURRAX T25, IKA®-Werke GmbH & CO. KG, 79219 Staufen, Germany) and sonicated (SONOPLUS HD 2070, BANDELIN electronic GmbH & Co. KG, 12207 Berlin, Germany) for 10 min on cycle 5 (0.5s pulse+0.5s pause) using 50% power. After cell disruption the remaining cell parts were removed by centrifugation (Avanti J-26XP centrifuge, rotor JA 25.50, Beckman-Coulter GmbH, 47807 Krefeld, Germany) and the supernatant was filtered through a 0.45µm syringe filter. The remaining supernatant was loaded onto a self-packed Ni-NTA column. The impurities were washed off with 10-15 column volumes of washing buffer (20mM Tris pH 7.5, 100mM NaCl, 40mM Imidazole). The protein was eluted with five column volumes of elution buffer (20mM Tris pH7.5, 100mM NaCl, 250mM Imidazole). The solution was dialyzed overnight against 2L dialysis buffer (20mM Tris pH 7.5, 100mM NaCl) in a 12-14kDa cut-off dialysis bag to get rid of the imidazole. For the dialyzed samples a size exclusion (SEC) had to be done. Therefore the protein solution was concentrated to 10ml using a centrifuge concentrators (Merck, Millipore, Billerica, USA) with a 10kDa cut off. The size exclusion was performed using Superdex 200 resin (Pharmacia XK 26, GE Healthcare, Solingen, Germany) packed in a 250 ml column. A flow rate of 2ml/min was used and 2ml samples were collected. The oligomeric state could be determined by comparison to a gel filtration standard (Bio-Rad Laboratories Ltd., Hemel Hempstead, UK). The monomeric fractions were pooled and subsequently concentrated for crystallization, using 10kDa cut-off centrifuge concentrators, for crystallization. For the crystallization fresh samples were used directly after the purification process if available, otherwise frozen samples were used. Frozen samples were stored at -80°C.

2.3.2. s-YJU3p

The purification of s-YJU3p was analogue to that of bMGL, although the used buffers were different.

Table 1 Buffer solutions for YJU3 L175S Q264R purification

Wash buffer	20mM Tris pH 8.0, 100mM NaCl, 40mM Imidazole
Elution buffer	20mM Tris pH 8.0, 100mM NaCl, 250mM Imidazole, 5% Glycerol)
Dialysis buffer	20mM Tris pH 8.0, 100mM NaCl, 5% Glycerol, 1mM DTT, 1mM EDTA

2.4. s-YJU3p Activity Assay with the JZL 184 Inhibitor

To test if JZL 184 is inhibiting s-YJU3p in spite of its large size compared to the other inhibitors (Figure 5) a MGL hydrolase activity assay was performed. Purified protein was dialyzed overnight to get rid of glycerol, because the free glycerol generated during the reactions was measured using a commercially available glycerol detection kit (Sigma Aldrich, St. Louis, USA). s-YJU3p was rebuffered into potassium phosphate buffer (100mM, pH7.24) using a desalting column. The C18 substrate (1-Oleoyl-*rac*-glycerol) was dissolved in chloroform to a concentration of 5mg/mL and 1mL was dried in N_2 stream and dissolved in 240µL MilliQ water and 1100µL of potassium phosphate buffer (100mM, pH 7.24) by sonicating it (SONOPLUS HD 2070, BANDELIN electronic GmbH & Co. KG, 12207 Berlin, Germany) at cycle 3 (0.3s pulse + 0.7s pause) till the solution got turbid. Then it got complexed with 660µL BSA (20%) to a molar ration of 1:1 and again sonicated like before until the solution cleared up. For the assay itself 10µL of protein with a concentration of 2ng/µL were incubated with 100µL of substrate at 37°C for 20 minutes and then stopped by adding 100µL of chloroform and intense mixing. The samples were spun for 10 minutes (Centrifuge 5415R, Eppendorf AG, Hamburg Germany) at 16.1g and 50µL of the aqueous phase were mixed with 200µL of free glycerol reagent. The mixture was again incubated for 10min at 37°C and then the absorption at 497nm was measured using a plate reader (Biotrak II Visible Plate Reader, GE Healthcare, Solingen, Germany)(*33*). A standard curve was measured to determine the concentration of the free glycerol in the samples. As a positive control s-YJU3p without JZL 184 was used and as a negative control s-YJU3p was boiled for at least 15minutes to ensure its inactivity.

2.5. Crystallization

Crystallization setups were either performed in hanging drop or sitting drop mode. The hanging drop crystallization setups were carried out manually, the sitting drop

crystallizations were mostly done with an Oryx8 crystallization robot (Douglas Instruments Ltd, Berkshire, United Kingdom). The drop sizes for crystallization varied from 0.8µl in sitting drop setups (using the oryx8 robot) to 5µl in manual hanging drop set ups. Typical sizes were of 1.5µl for sitting drop and 3µl for hanging drop crystallization. For bMGL I145G and bMGL I145S the temperature for crystallization was varied from 16°C to 37°C. s-YJU3p crystallizations were typically set up at 20°C. This was done either in the previously known crystallization condition to obtain free form crystals for soaking experiments or in sparse matrix screens and optimizations, mixed with different inhibitors, for cocrystallization attempts.

2.5.1. bMGL I145S and bMGL I145G

Prior experience in our group with bMGL led to the assumption that bMGL I145S and bMGL I145G might crystallize in a similar condition as a previously crystallized bMGL complex. Different optimization attempts of a condition containing 0,1M citric acid pH 5.5 and 20% w/v PEG3000 (condition A2 from JCSG+ screen) led to crystalline objects in different drops ranging from oils to needle clusters at 20°C. These optimized conditions were then further varied, in regard to crystallization setups, temperature, concentration of protein and the volume of the condition in the reservoir, until diffracting crystals could be obtained. For bMGL I145G diffracting crystals could be obtained using hanging drop crystallization with 500µl reservoir solution in a condition containing 0.1M citric acid pH 5.8 and 22% w/v PEG3000 at 30°C. For bMGL I145S a different crystallization approach was taken. bMGL I145S was concentrated to ~45mg/ml and set up in a hanging drop plate with the condition 0.1M citric acid pH 5.8 and 22% w/v PEG3000 containing 200µl of reservoir solution. The final protein concentration ranging from 7mg/ml to 22mg/ml with crystals appearing in drops containing 18mg/ml to 19mg/ml. These crystals appeared in less than a week yet diffracted only to a low resolution (5-10Å).

2.5.2. s-YJU3p Inhibitor Complex

The first crystal of s-YJU3p was obtained by using a statistical screen, namely the Morpheus screen (Molecular Dimensions, Suffolk, UK) with ~16mg/ml protein. The specific condition was Morpheus C5 condition (10% w/v PEG 20000, 20% w/v PEGMME 550, 0.09M NPS mix [0.03M Sodium nitrate, 0.03M Sodium phosphate dibasic dihydrate and 0.03M Ammonium sulfate] and 0.1M MOPS/HEPES pH 7.5.). This drop was used to prepare a seeding stock using a seed bead and the protocol provided by Douglas Instruments. The seeding stock (diluted 1:1000) was again used

to seed a Morpheus screen and a weakly diffracting crystal could be obtained, by members of our group, in the condition C9 (10% w/v PEG 20000, 20% w/v PEGMME 550, 0.09M NPS mix and 0.1M Bicine/Trizma pH 8.5). This crystal was again made into a seeding stock and was the basis for my soaking and co-crystallization attempts. Two different approaches were chosen, the first one was co-crystallization with different Inhibitors (Chapter 2.5.2.2) and the second one was soaking of free form s-YJU3p crystals with inhibitors (Chapter 2.5.2.1).

2.5.2.1. s-YJU3p Soaking

To obtain free form s-YJU3p crystals for soaking attempts hanging drop plates with the previously known crystallization condition(10% w/v PEG 20000, 20% w/v PEGMME 550, 0.09M NPS mix and 0.1M Bicine/Trizma pH 8.7), used for the successful crystallization of s-YJU3p, were set up. In a hanging drop setup 2µl of s-YJU3p (~14mg/mL) were mixed with 2µl of the crystallization condition and 1µl of seeding stock. The free form crystals appeared within two weeks in most of the drops. Crystals were harvested and transferred to 1.5µl of stabilization solution (20% [w/V] PEG 20000, 40% [V/V] PEG 550 MME) 0.5µl of substrate analog, with a concentration of 50mg/ml. The crystals were soaked for at least 20 minutes followed by shock freezing in liquid nitrogen. Then the crystals were tested for diffraction using the in house X-ray source (Microstar, Bruker, Karlsruhe, Germany) with a MAR 345 detector (Marresearch Gmbh, Norderstedt, Germany).

2.5.2.1.1. Crosslinking

In order to enhance the resolution of the soaked crystals, gentle crosslinking with glutaraldehyde was applied (*38*). A Micro-Bridge with a 2µl drop of 25% glutaraldehyde was placed in the reservoir of the hanging drop plate after the crystal soaking. The crystal, still in the stabilization solution, was placed for at least 30 minutes over the Micro-Bridge.

2.5.2.2. s-YJU3p Cocrystallization

0.36mmol (~15mg) of s-YJU3p were mixed with different inhibitors and substrate analogues dissolved in 99% EtOH at a molar ration of 1:5 (YJU3p: inhibitor) with a typical concentration of the inhibitor of 50mg/mL. The mixture was incubated at 4°C for at least one hour. Then the protein solution was diluted 1:10 two times with crystallization buffer (20mM Tris pH 8.0, 100mM NaCl, 5% Glycerol, 1mM DTT and 1.5mM EDTA) and concentrated to original volume using centrifuge concentrators

(Merck Millipore, Billerica, USA). Precipitated protein from the dilution and concentration steps were separated by centrifugation (10 min at 16.1g (Centrifuge 5415R, Eppendorf AG, Hamburg Germany) in order not to disturb the crystallization process. Therefore the protein solution was spun down for 10 min using a table centrifuge (Centrifuge 5415R, Eppendorf AG, Hamburg Germany) at 16.1g. The resulting s-YJU3p-inhibitor solution was used to set up multiple sparse matrix screens and optimizations.

2.6. Structure Determination

2.6.1. X-Ray Diffraction

All crystals were first tested on our rotating anode (Microstar, Bruker, Karlsruhe, Germany) to verify they were not salt and then stored in liquid nitrogen for measurement at a synchrotron facility. The crystals were measured either at DESY (Hamburg, Germany), ELETTRA (Trieste, Italy) or at ESRF (Grenoble, France). The high intensity X-ray beams at these synchrotron facilities give us the possibility to record datasets much faster, in a time range from minutes to hours as opposed to days on the rotating anode.

2.6.2. Data Processing and Refinement

All datasets were indexed and integrated using iMosflm(*39*), the data was merged and scaled either by using Pointless and Scala or aimless (*40*), which also includes Pointless and a replacement for Scala(*41*). The solution of the phase problem could be done by Molecular replacement using MOLREP (*42, 43*). The refinement was done by using Refmac5 (*34*). Coot (*35*) was used for the manual model building and refinement, for tasks going beyond the abilities of Refmac5. Molecular graphics were created using PyMOL(*36*).

2.6.2.1. bMGL I145S and bMGL145G

Diffracting crystals could be obtained yet no dataset, sufficient to determine the structures of these variants, could be collected.

2.6.2.2. s-YJU3p Complex Crystals

2.6.2.2.1. s-YJU3p Cocrystallization

The s-YJU3p -C20 (2.5Å) complex datasets were indexed and integrated using iMosflm (*39*). Scaling and merging was done using Aimless and molecular replacement was done using MOLREP (*42, 43*) with a structure of a free form s-YJU3p, previously solved by Philipp Aschauer (paper in preparation). Refmac5 was used to perform rigid body and restrained refinement cycles, followed by modifying the model and inserting missing parts and solvent manually using Coot.

2.6.2.2.2. s-YJU3p Soaking

Datasets obtained from soaking experiments were treated similar to the datasets from co-crystallization, yet in some cases, Pointless and Scala were used instead of Aimless(*40, 41*). For some of these datasets the C20 co-crystal structure was used for molecular replacement.

3. Results

3.1. Purification

The success of protein expression and purification was tested by SDS polyacrylamide electrophoreses and by size exclusion chromatography (Chapter 2.3.1).

3.1.1. bMGL

For bMGL, after the purification with Ni-column and dialysis, a size exclusion chromatography step was necessary. Previous experiments have shown that bMGL is mostly in a monomeric state, yet a small oligomeric peak is also present which can be separated by size exclusion chromatography.

3.1.1.1. bMGL I145S

In figure 14 a typical gel of a bMGL I145S purification is shown. It can be seen in lane 8 and 9 that bMGL could be purified very well.

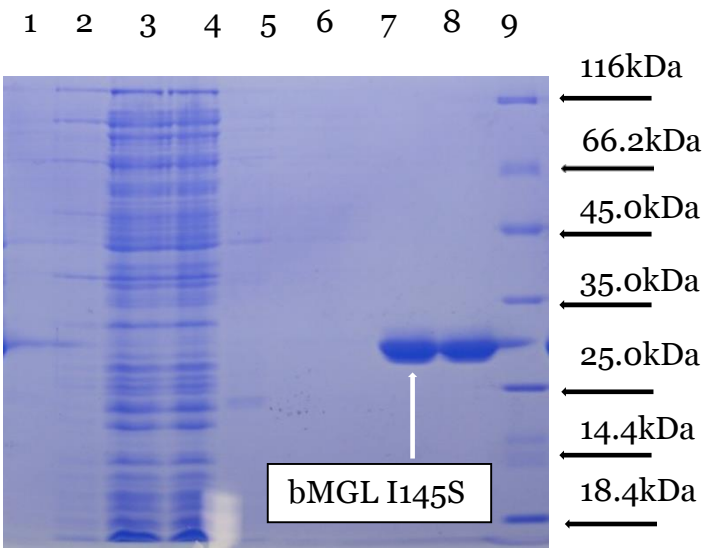

Figure 14 Typical gel from a bMGL I145S Purification

1: Loading fraction 1
2: Loading fraction 2
3: Loading fraction 3
4: Washing fraction 1
5: Washing fraction 2
6: Washing fraction 3
7: Elution fraction 1
8: Elution fraction 2
9: Elution fraction 3
10: Unstained protein marker

3.1.1.1. bMGL I145G

A typical gel from a bMGL I145G purification using the methods described in chapter 2.3.1 (Figure 15).

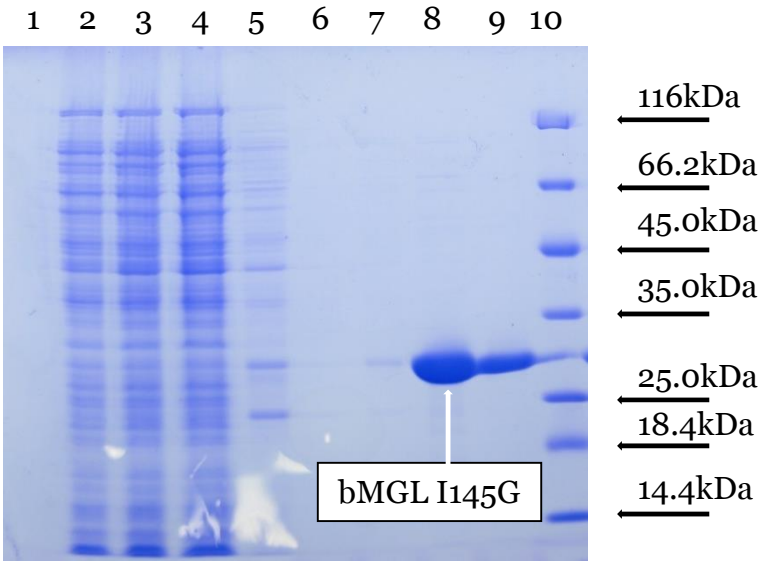

Figure 15 Typical gel from a bMGL I145G purification

1: Loading fraction 1
2: Loading fraction 2
3: Loading fraction 3
4: Washing fraction 1
5: Washing fraction 2
6: Washing fraction 3
7: Elution fraction 1
8: Elution fraction 2
9: Elution fraction 3

3.1.2. s-YJU3p

s-YJU3p was monitored after the expression and purification process by SDS page and size exclusion chromatography (Figure 16, 17). After the oligomeric state was determined only monomeric protein was used for crystallization setups.

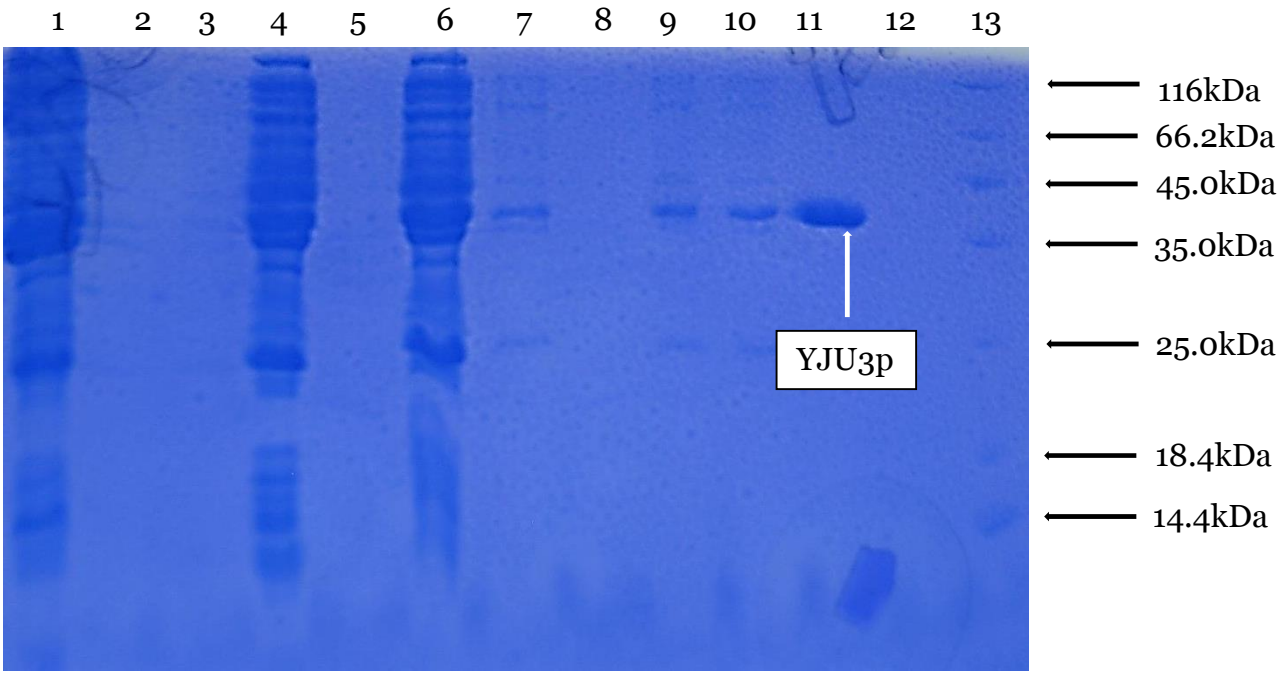

Figure 16 Typical gel from a s-YJU3p purification

1: Pellet
2: Supernatant
3: Empty
4: Beginning of loading
5: End of loading
6: Beginning of washing
7: End of washing
8: Empty
9: First elution fraction
10: Second elution fraction
11: Third elution fraction
12: Empty
13: Unstained protein marker

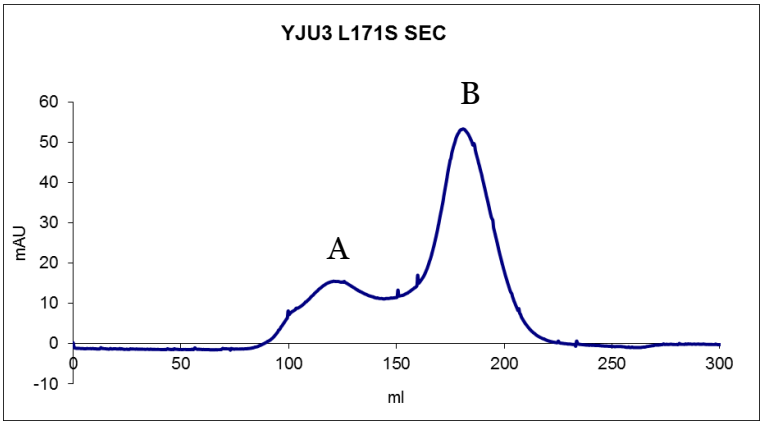

Figure 17 Typical size exclusion chromatogram from YJU3. Aggregate (A) monomer (B)

3.2. YJU3p-JZL 184 Activity Assay

It couldn't be shown in the activity assay that s-YJU3p is actually inhibited by JZL 184. Although a trend is recognizable (Figure 18), a students t-test did not show that the difference in measured activity in the assay was significant.

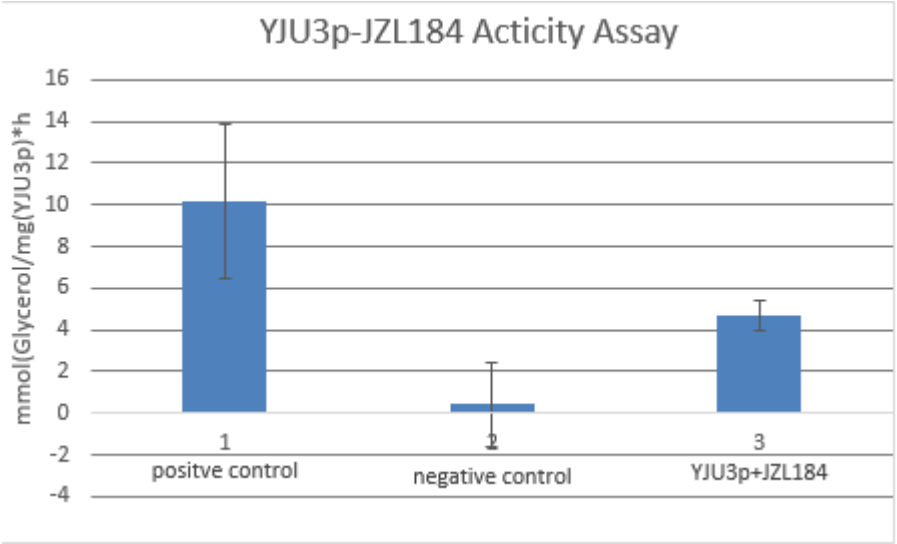

Figure 18 Results of MG hydrolase assay. Positive control YJU3p, negative control YJU3p boiled for at least 10 minutes.

3.3. Crystallization and Data Collection

3.3.1. bMGL I145S and bMGL I145G

Due to prior knowledge from crystallizing bMGL, optimizations of the original crystallization conditions were set up (Chapter 2.5.1)(*31*). Diffracting crystals of both bMGL variants could be obtained (Figure 19, 20, 27, 28).

3.3.1.1. bMGL I145G

Diffracting crystals could be obtained and measured on the rotating anode (Chapter 2.6). Due to the low diffraction quality of these crystals it was decided not to record data sets at a synchrotron (Figure 19, 20).

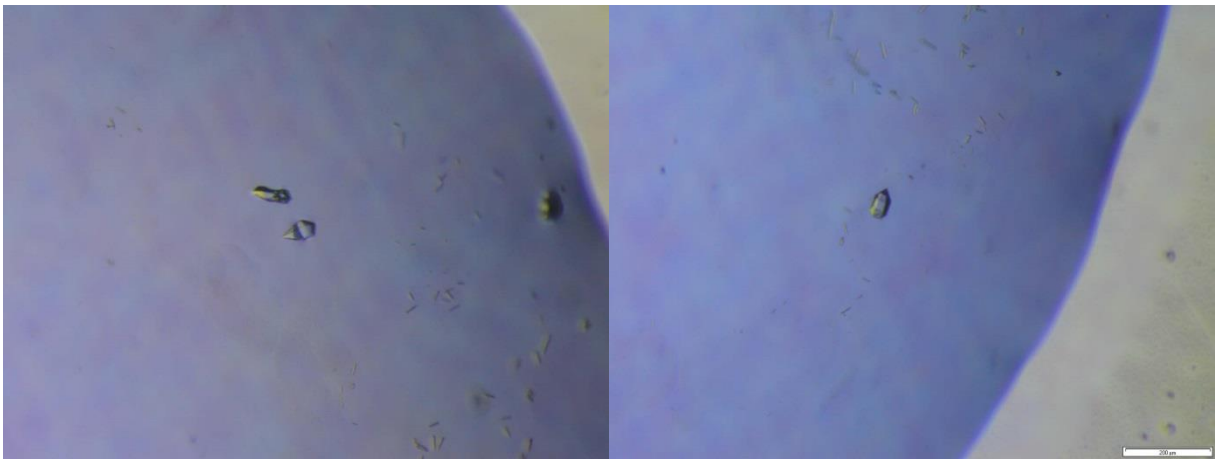

Figure 19 Crystals of bMGL I145G. Crystallization setup in the condition containing 0,1M citric acid pH 5.8 and 22% w/v PEG3000 at 30°C 500µl reservoir solution

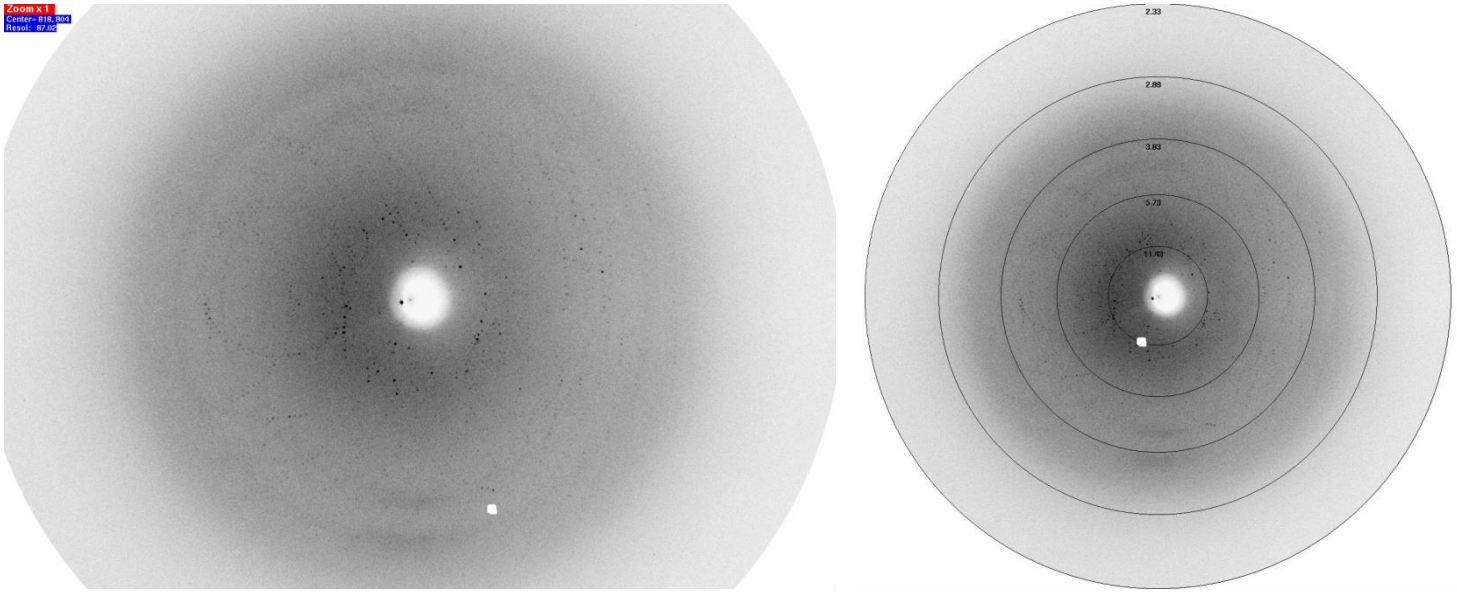

Figure 20 Diffraction patterns of bMGL I145G with (right) and without (left) resolution rings. Diffraction patterns can be seen up to 5Å.

Although during the experimental work for my thesis, the structure for bMGL I145G could not be solved, the structure could be determined later on in our lab (unpublished data, Krishna Mohan Padmanabha Das, Structural Biology, KFU-Graz). The crystal was grown in the condition pH6.5, 0.1M amino acids, 0.1M Buffer System 1,

37.50%[v/v] MPD P1K P3350 (Figure 21). Additionally some NMR studies have been

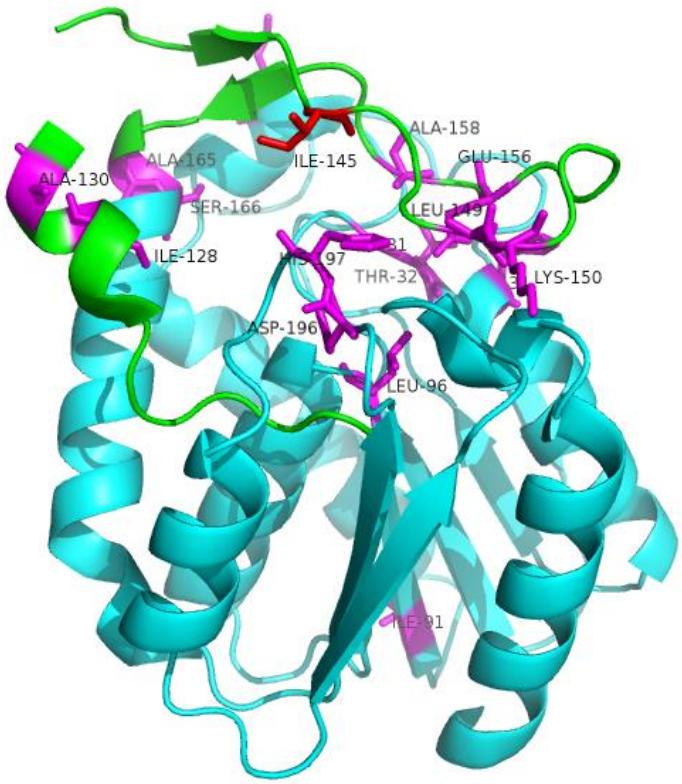

Figure 23 Cartoon representation of bMGLI145G. The cap is shown in green and the α/β hydrolase core in blue. Residues that ate shifted according to NMR are shown in stick representation (magenta). The cap residue isoleucine 145 in the free form structure is highlighted in red.

performed to further enhance the knowledge gained by crystallography (Chapter 7.1 short description). In the HSQC spectrum shown in Figure 22 the pink peaks belong to the free form bMGL and the blue peaks are from the I145G variant. The shifted amino acids have been mapped in the comic representation of bMGL I145G. It can be seen that the shifted amino acids are mostly in the cap region or directly adjacent to the cap region (Figure 23).

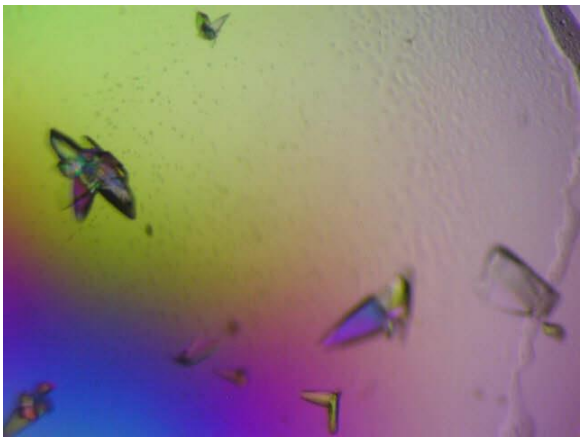

Figure 21 Crystal used for recording the dataset for bMGL I145G. (Kindly provided by Krishna Mohan Padmanabha Das)

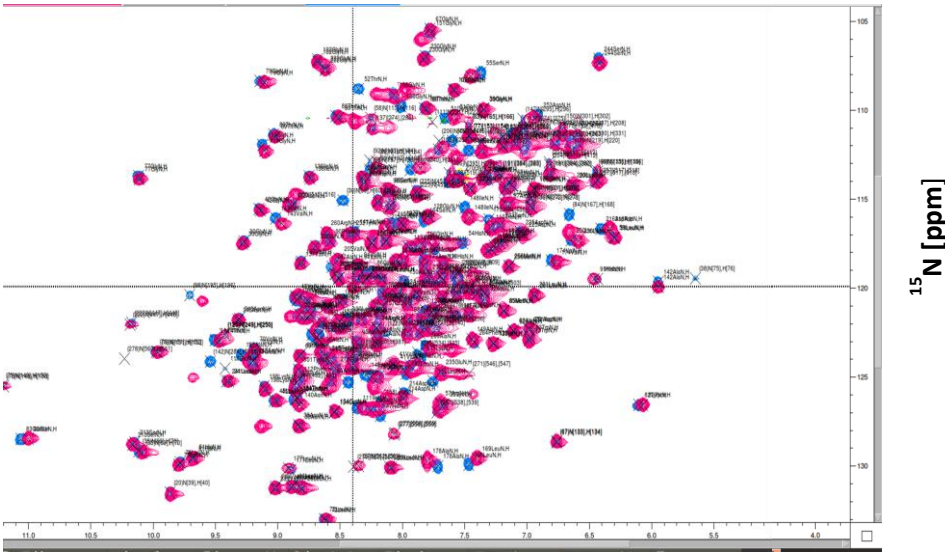

Figure22 Comparison of 15N HSQC of the free form (pink) and the I145G variant (blue) of bMGL. (Kindly provided by Krishna Mohan Padmanabha Das)

3.3.1.2. bMGL I145S

Crystals showing low resolution diffraction could be obtained (Chapter 2.5.1, Figure 24, 25) and were measured on the rotating anode (Chapter 2.6). Due to the low resolution of this diffraction patterns it was decided not to collect data sets at a synchrotron facility.

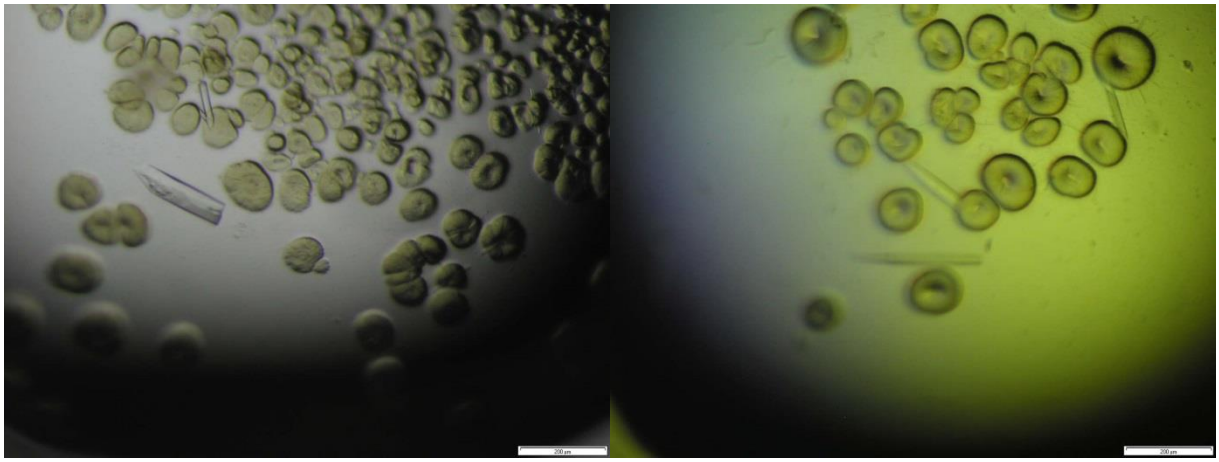

Figure 24 Crystals of bMGL I145S. Crystallization setup in the condition containing 0,1M citric acid pH 5.8 and 22% w/v PEG3000 and 200µl of reservoir solution

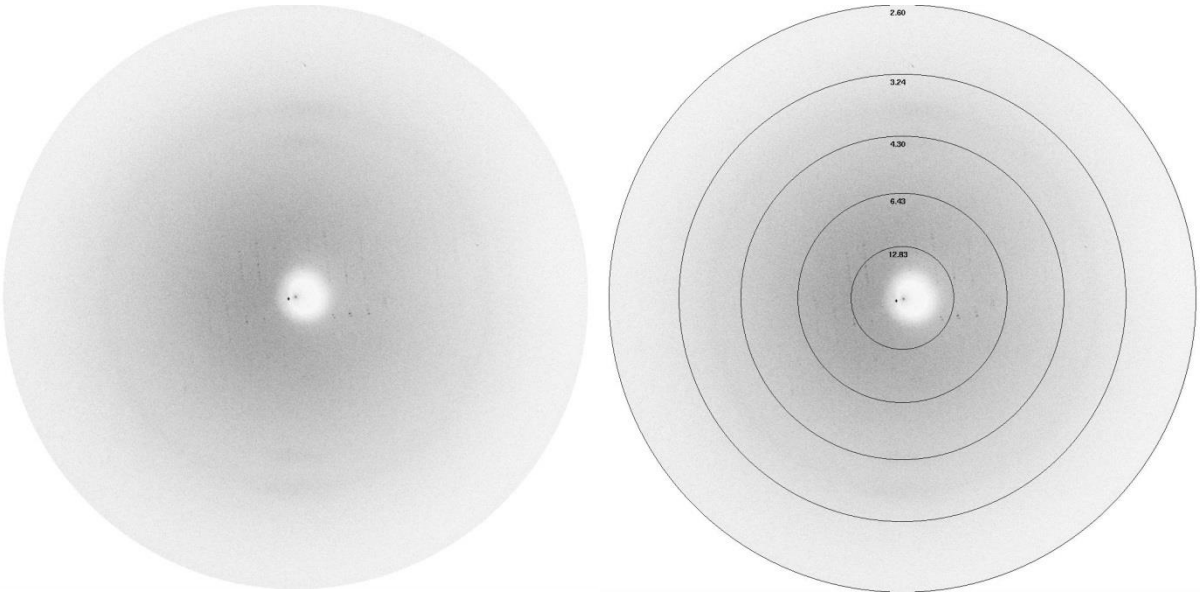

Figure 25 Diffraction pattern of bMGL I145G with (right) and without (left) resolution rings. Diffraction can be seen to a resolution of about 8Å

3.3.2. s-YJU3p

3.3.2.1. Soaking Experiments

As described in chapter 2.5.2.1, free form crystals of s-YJU3p (Figure 26) have been soaked with inhibitors and substrate analogues and were tested on the home source for diffraction. Crystals of sufficient diffraction quality on the home source were sent to a synchrotron facility and measured. For every substrate analogue (C14, C16, C18, C20,

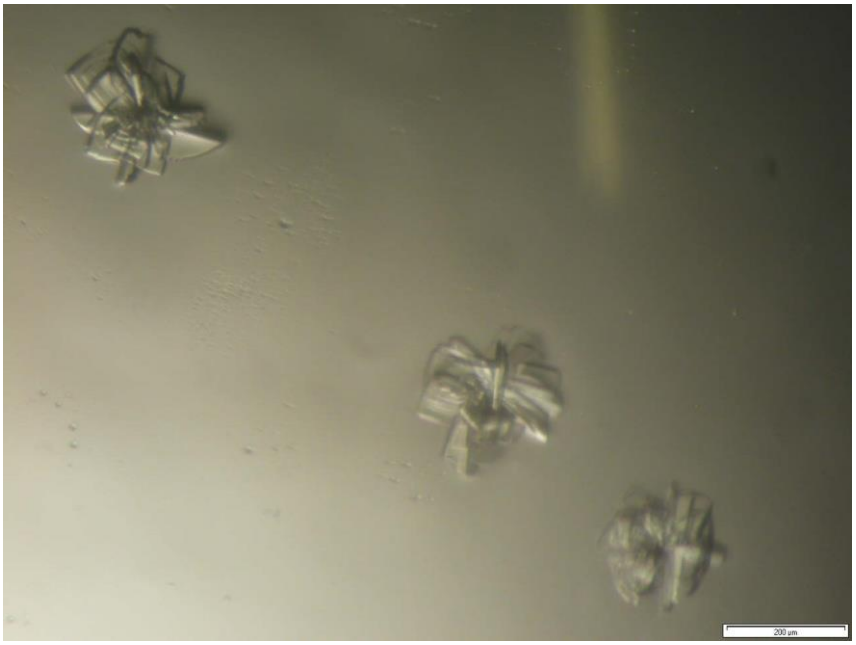

Figure 26 s-YJU3p crystals used for soaking experiments

PMSF, JZL-184) at least one diffracting crystal could be measured. Free form s-YJU3p crystals were grown (Chapter 2.5.2.1) and soaked with substrate analogue. In general the soaked crystals diffracted only to a lower resolution compared to free form crystals. Therefore some of the soaked crystals were crosslinked (Chapter 2.5.2.1.1) as an attempt regain high diffraction. In these experiments no improvement of the resolution could be shown in regard to non-crosslinked (Chapter 2.5.2.1.1).

3.3.2.1.1. Soaking s-YJU3p with C14, C16, C18 and C20 Substrate Analogue

As mentioned above, at least one crystal could be measured for every substrate analogue used. Data sets were collected at synchrotron facilities, processed and refined (Chapter 2.6). Only at a very late stage of the refinement process it became clear that due to low resolution of the datasets and maybe just a partial occupation of the substrate analogue in the crystal, it is not possible to unambiguously determine if the protein really is covalently linked to the substrate analogue. Even in the C14 soaked data set, showing the best electron density, suspected to be from the substrate analogue, which diffracted only to a resolution of 3.41Å, after the refinement it couldn't be proven with enough certainty that the inhibitor is present in the structure (Figure 27). For the other datasets that have been refined there was even less electron density and therefore no way of determining if the substrate analogue was present in the structures. At first it was assumed that a gap in the cap-region, between Ile166 and Met159 (Figure 28), that could be seen in all soaking datasets was a clue that the soaking experiments did in fact work as planned. But only after closer examination of already solved datasets, it turned out that this gap is present in all structures of s-YJU3p even in the free form structure.

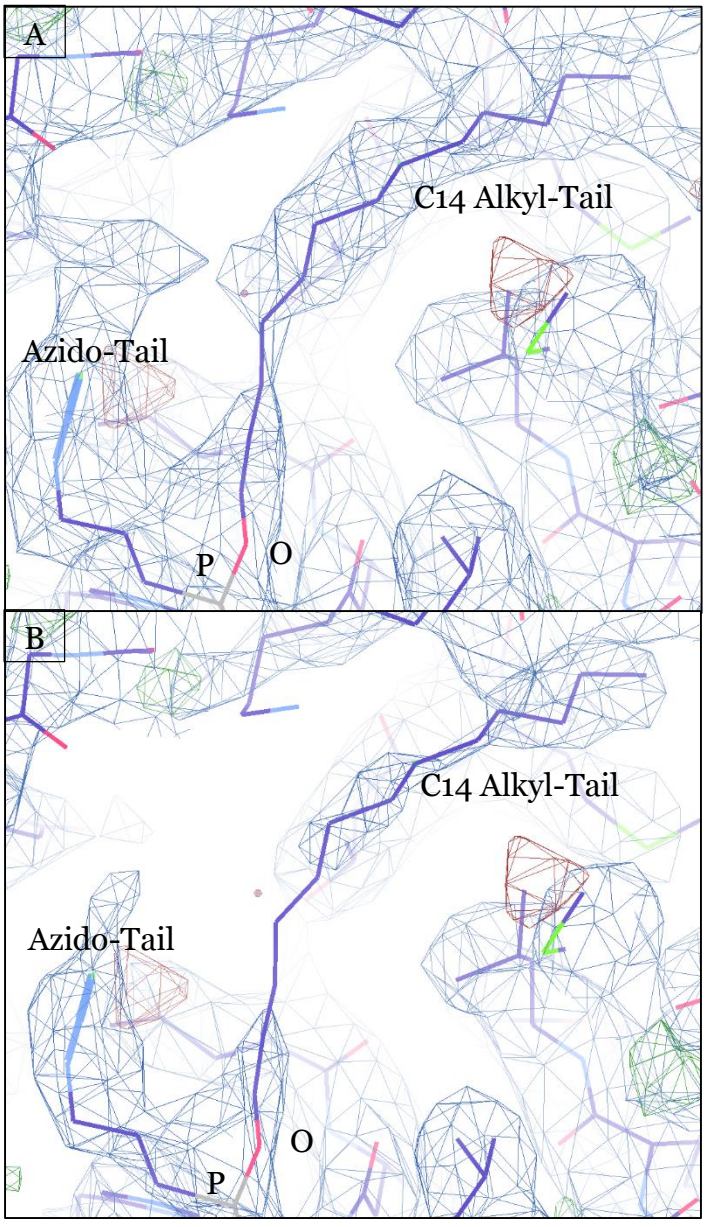

Figure 27 C14 substrate analogue fitted into the electron density map (Fo-Fc) of C14 substrate analogue soaking. Red blobs are negative and green blobs positive electron density (2Fo-Fc) (A) Sigma cut-off 0.5 (B) Sigma cut-off 1 [Figure taken in Coot]

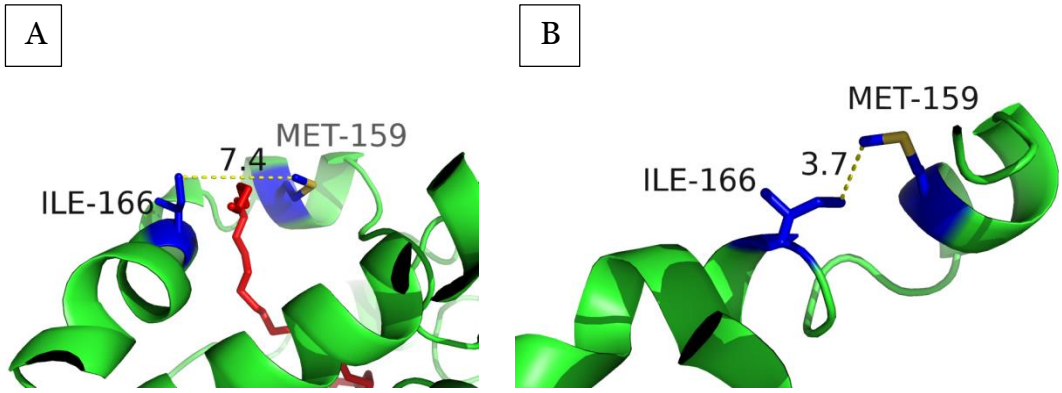

Figure 28 Gap in the cocrystal-structure of s-YJU3p bound to C20 substrate analogue (A) compared to free form structure (B).

3.3.3. s-YJU3p Cocrystallization

s-YJU3p cocrystallization attempts were performed with all available inhibitors and substrate analogues with varying degree of success. For the substrate analogues called C14 and C16 (Chapter 1.4) and for the commercially available serine hydrolase inhibitor JZL184 no crystals could be obtained, for C18 and PMSF crystals have been grown, harvested and tested at the rotating anode but they did not show any diffraction (Figure 30).

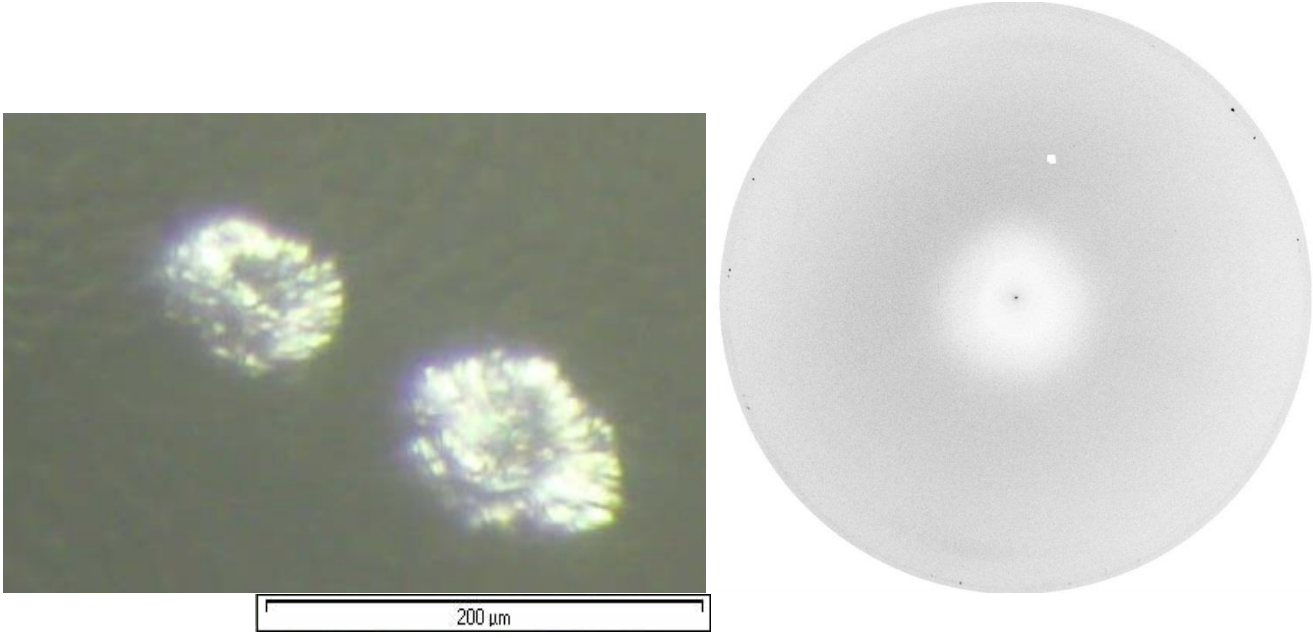

Figure 30 Non diffracting s-YJU3p – PMSF crystals

Only for the substrate analougue called C20 a crystal could be obtained that diffracted well enough to collect a dataset and solve the structure (Figure 31, 32).

The crystal diffracted to 2.5Å which proofed to be sufficient to solve the structure with adequat R-values (Figure 31, 32)(Table 2,).

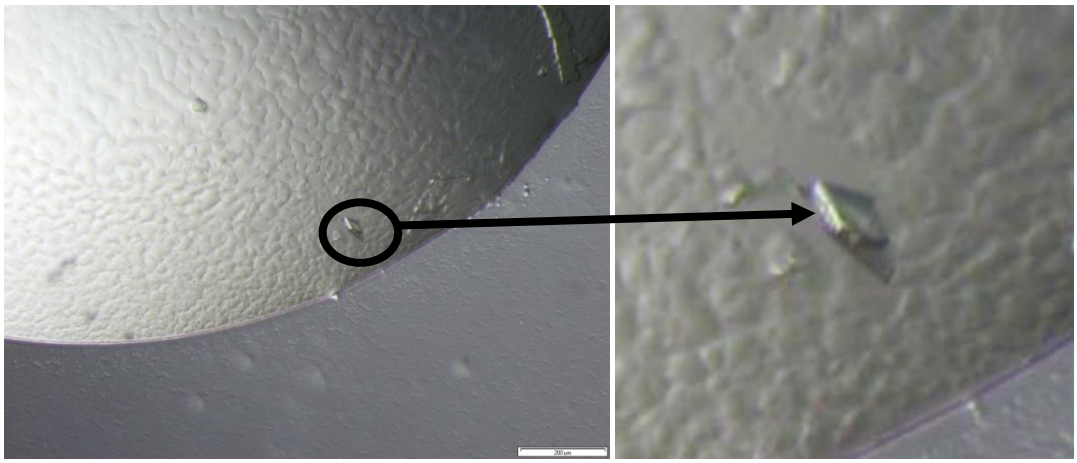

Figure 31 Diffracting C20 crystal used for structure solving.

Table 2 Processing and refinement statistics of s-YJU3p

s-YJU3p C20 analog complex ID-29 ESRF			
Measurement and processing			
Wavelength	0.97939Å		
Space Group	$P2_12_12_1$		
Unit cell	a	b	c
	76.76Å	107.1Å	165.5Å
Resolution	65.5Å-2.5Å		
	low resolution		high resolution
Resolution of shell	82.72 – 7.91		2.64 – 2.5
R_{merge}	0.052		0.965
CC 1/2	0.997		0.178
Completeness	99.2%		99.6%
Multiplicity	4.2		4.2
Mean I/sd(I)	18.3		1.8
Average mosaicity	0.58		
Refinement			
R_{free}	25.68%		
R_{work}	20.13%		
RMS bonds	0.004		
RMS angles	0.806		
Ramachandran favored	96.91%		
Ramachandran disallowed	0.33%		
Rotamer outlier	0.95%		
Wilson B-factor	43.76		
None solvent atoms	9807		
Solvent atoms	151		

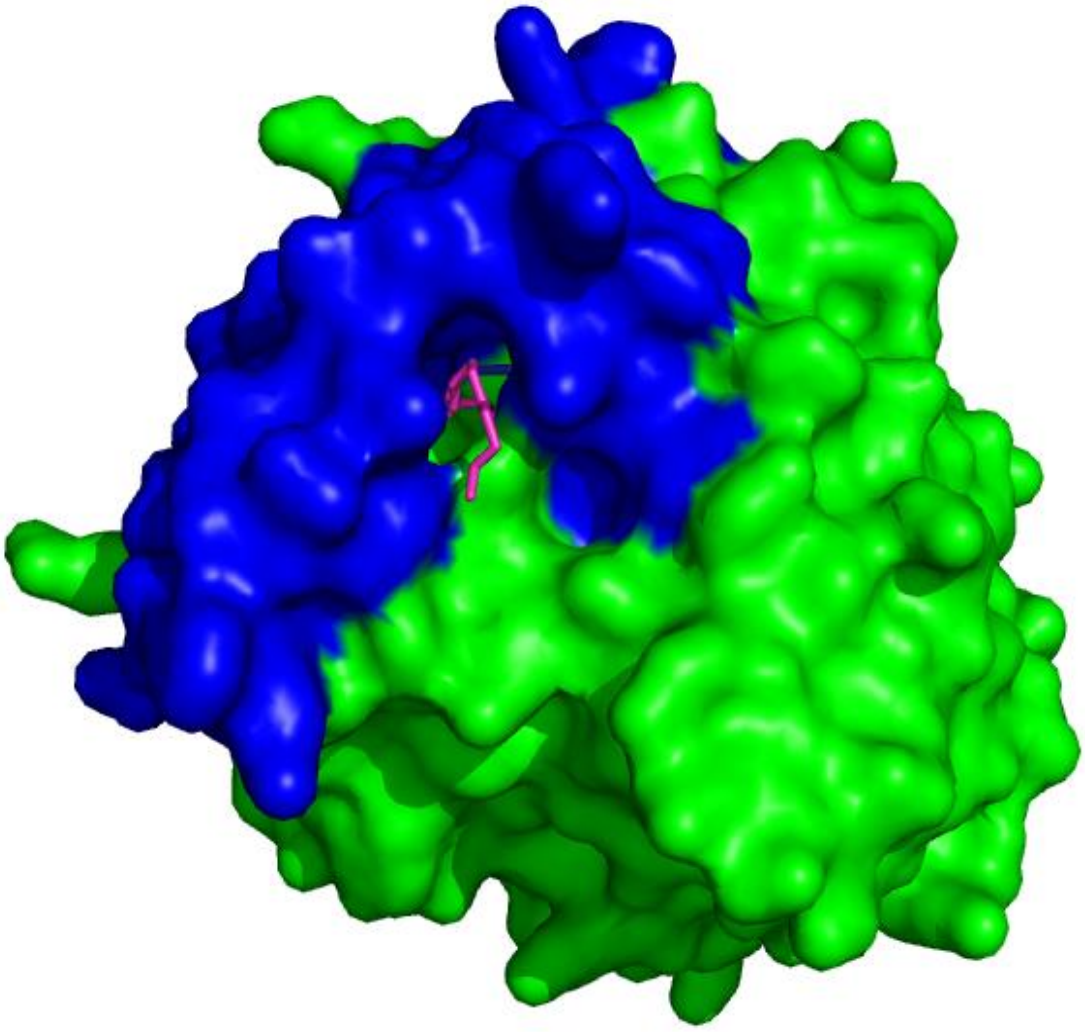

Figure 32 Surface view of s-YJU3p shows a slightly opened cap (blue) and the C18 Substrate analogue sticking out of the catalytic center (green).

4. Discussion

4.1. bMGL I145G

Upon further investigation of the bMGL I145G crystal structure provided by Krishna Mohan Padmanabha Das it can be seen that the shifted amino acids are not all in the near vicinity of the mutated residue (Figure 23) but they are mostly in the cap region or directly adjacent to the cap region. Although this finding is interesting, no difference in the backbone conformation can be seen when the crystal structure of the free form of bMGL is superimposed with the I145G variant (Figure 33).

A superposition of the bMGL I145G cap with the caps of the previously crystallized C14 (PDB 4KE7) and C18 (PDB 4KE9) substrate analogue complexes shows that there are some shifts in the backbone but mostly in the flexible parts of the cap region (Figure 34). As it can be seen in figure 34 the changes that can be seen in the crystal structures are restricted to rather small stretches. The missing part of the bMGL I145G in the cap region is also missing in almost all of the previously solved crystal structures of bMGL except for the C18 structure, this leads to the assumption that this part is very flexible, this is supported by the fact that it is also mostly unstructured.

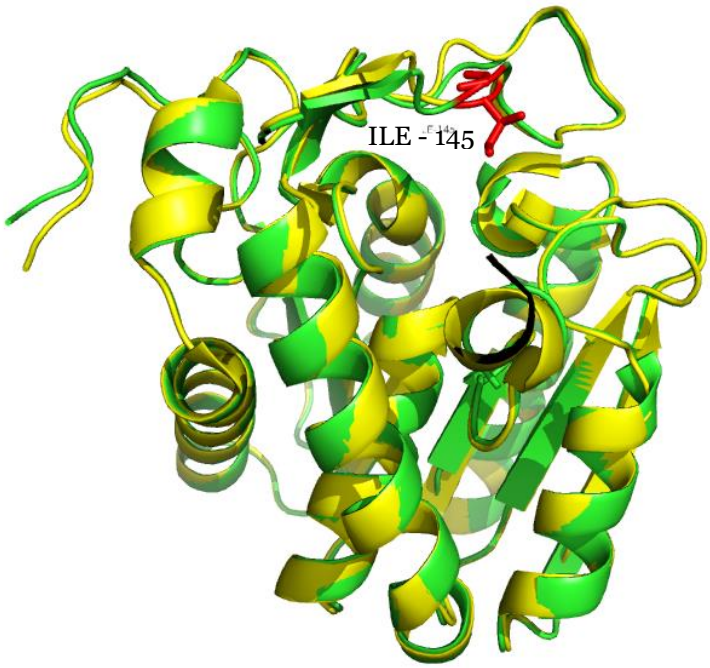

Figure 33 A superposition of bMGL in free form (Chain A, green/brown, PDB 3RLI) and bMGL I145G (magenta). Residue 145 is shown in both structures in stick representation and highlighted in red (Kindly provided by Krishna Mohan Padmanabha Das).

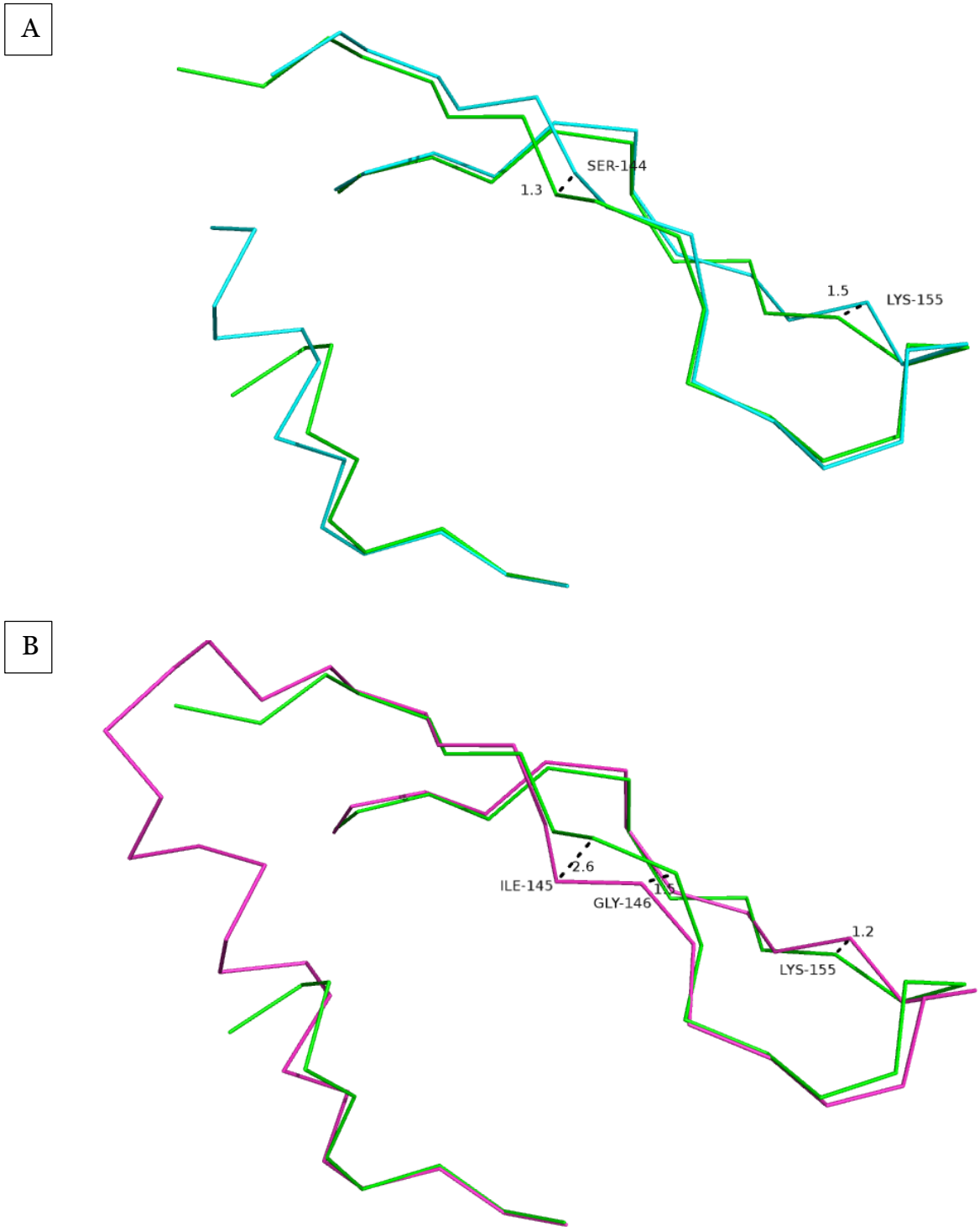

Figure 34 Superposition of (A) bMGL I145G (Chain A, green,) with the C14 substrate analogue bound form (Chain A, PDB 4KE7, purple) and (B) bMGL I145G (Chain A, green,) with the C18 substrate analogue bound form (Chain A, PDB 4KE9, magenta).

4.2. s-YJU3p

The major questions we investigated were structural. The complex was compared to structures and conformational changes of other MGLs, especially bMGL. In figure 35

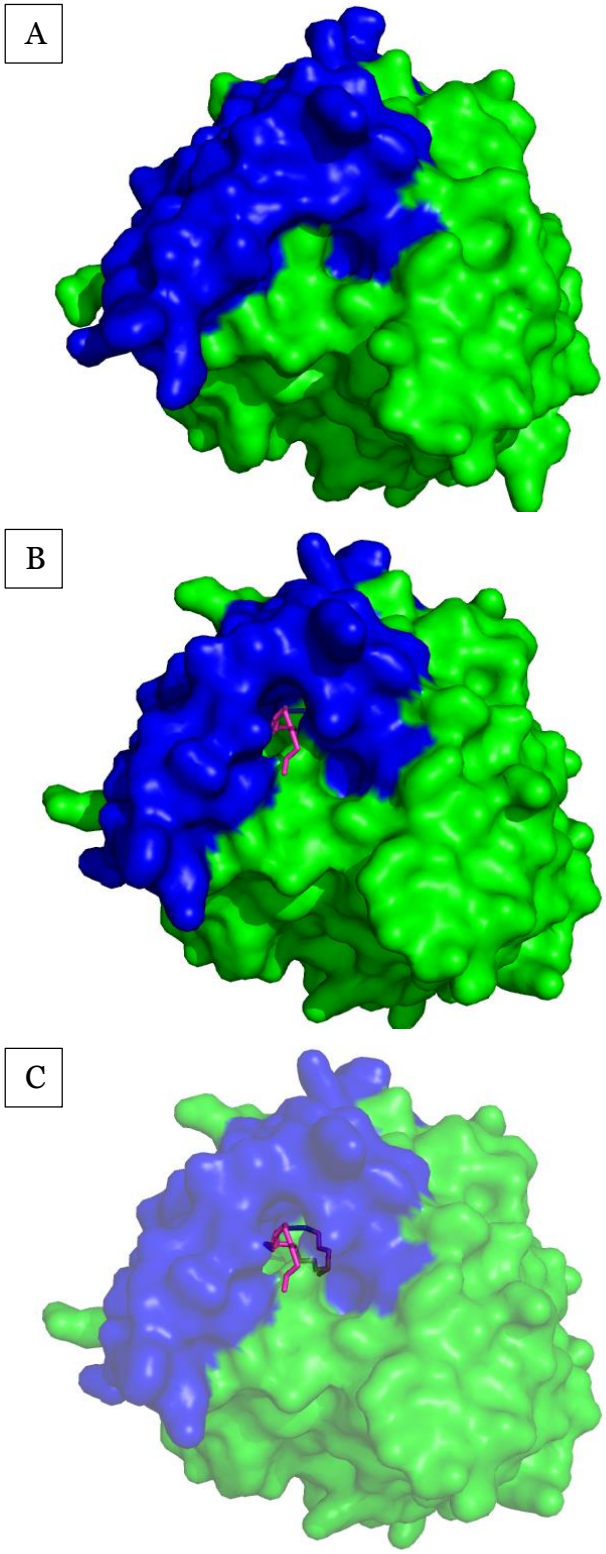

Figure 35 Surface representation of s-YJU3p in free form (A), inhibitor bound (B, C), and semi-transparent (C) inhibitor.

and 36 the closed free form structure of s-YJU3p and the substrate analogue bound form are compared in surface and cartoon representation. Only minor changes in the active center of s-YJU3p CRMSD 0.181Å) are seen whereas in the cap region the conformational changes are in a larger range (0.401Å). Nevertheless, there has to be an even larger movement in the cap structure, otherwise there would be no way for the substrate, or in this case the substrate analogue, to enter the active center of the enzyme with the nitro phenol ring still attached. The open form of s-YJU3p seems to appear in all structures. Further investigation showed that the backbone of s-YJU3p in the vicinity of the cap opening is shifted for a Maximum of 2.2-2.5 Å in a two amino acid stretch of Asp165 and Ile166 (Figure 37) compared to the free form closed structure. This shift is accompanied by small structural shifts in the range of 1.5Å in the direction the C terminus of the enzyme or more exactly at Ser175 and Thr182. The rest of the backbone in this area (Met159-Asp185) seems to be shifted

less than 1Å. Starting from amino acid 185 the backbone conformation again is the same as in the free form closed structure (Figure 37).

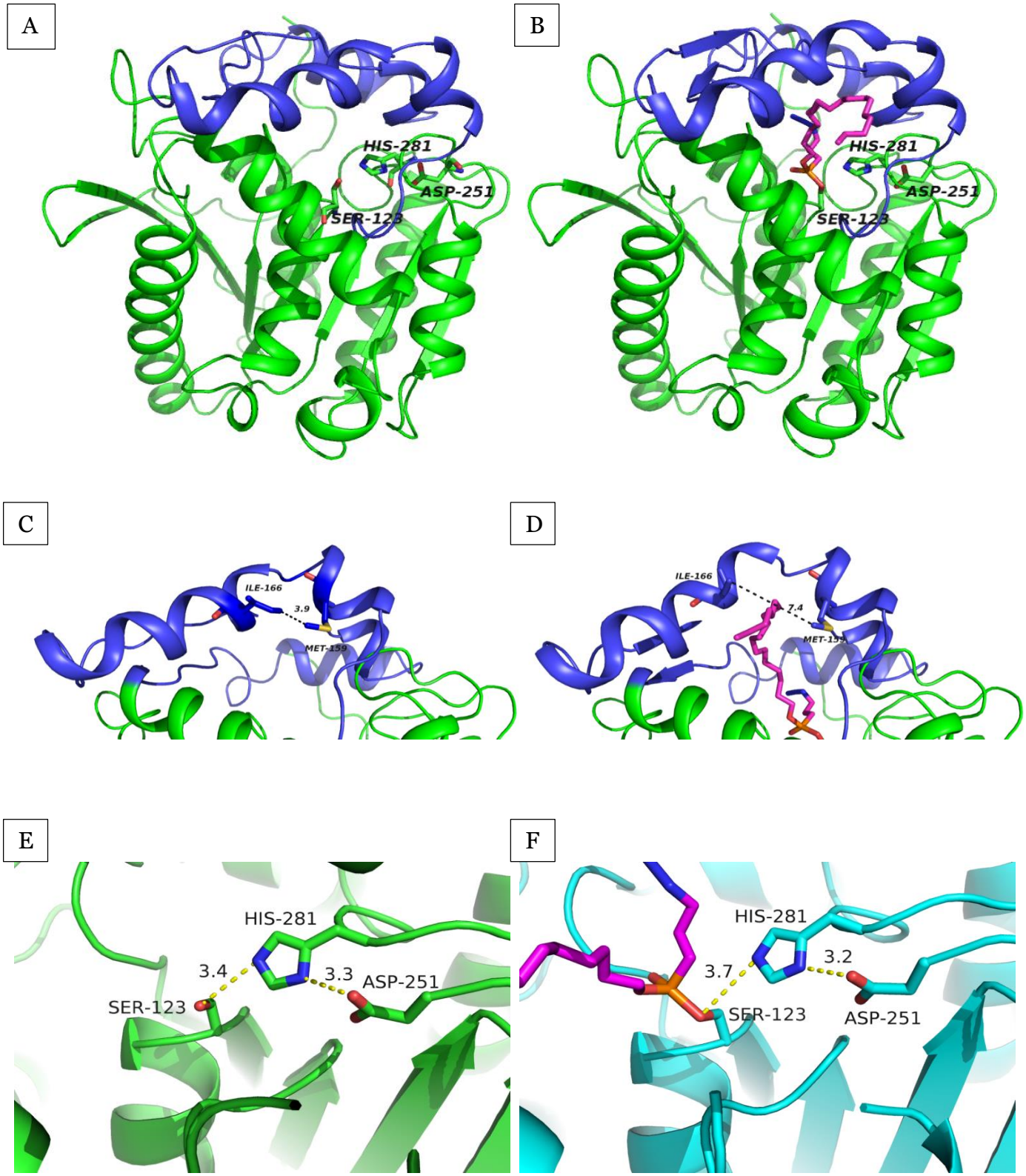

Figure 36 Overall comparison of un-complexed s-YJU3p in cartoon representation with the substrate analogue bound form (A, B), comparison of the cap-region (RMSD 0.401Å) (C, D) and the catalytic triad (E, F).

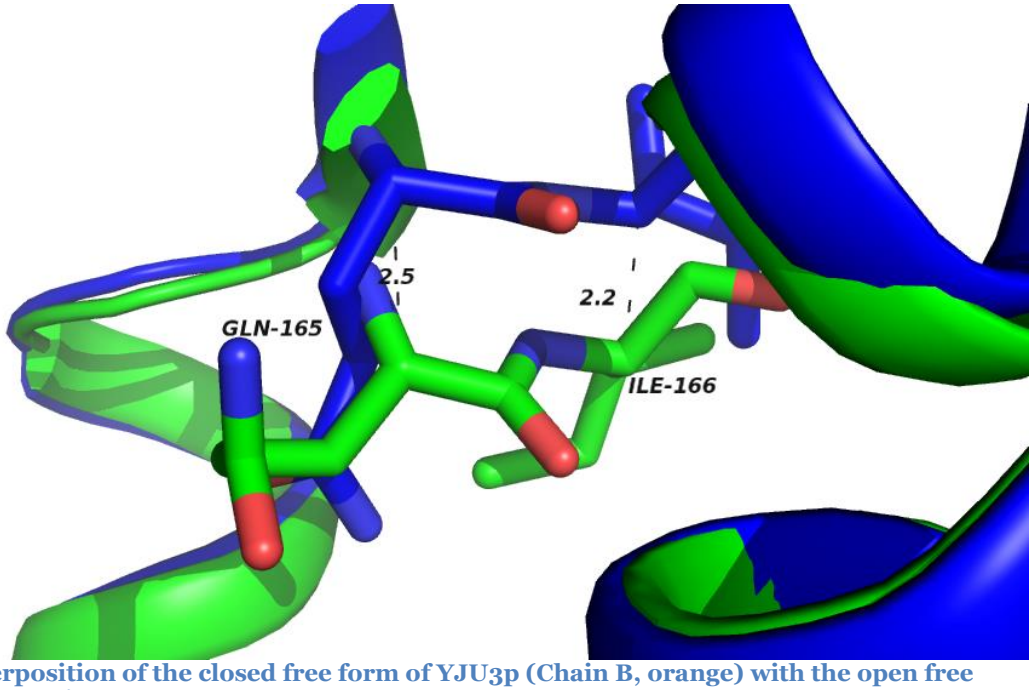

Figure 37 Superposition of the closed free form of YJU3p (Chain B, orange) with the open free form of YJU3p (Chain A, green)

A superposition of the free form open structure and the inhibitor bound open structure reveals that the only major difference occurs at the side chain of GLN165 where the C_δ of the sidechain is shifted or pushed outwards for about 5.3Å to provide enough space for the tail of the substrate analogue to fit through the opening (Figure 38, 39). There

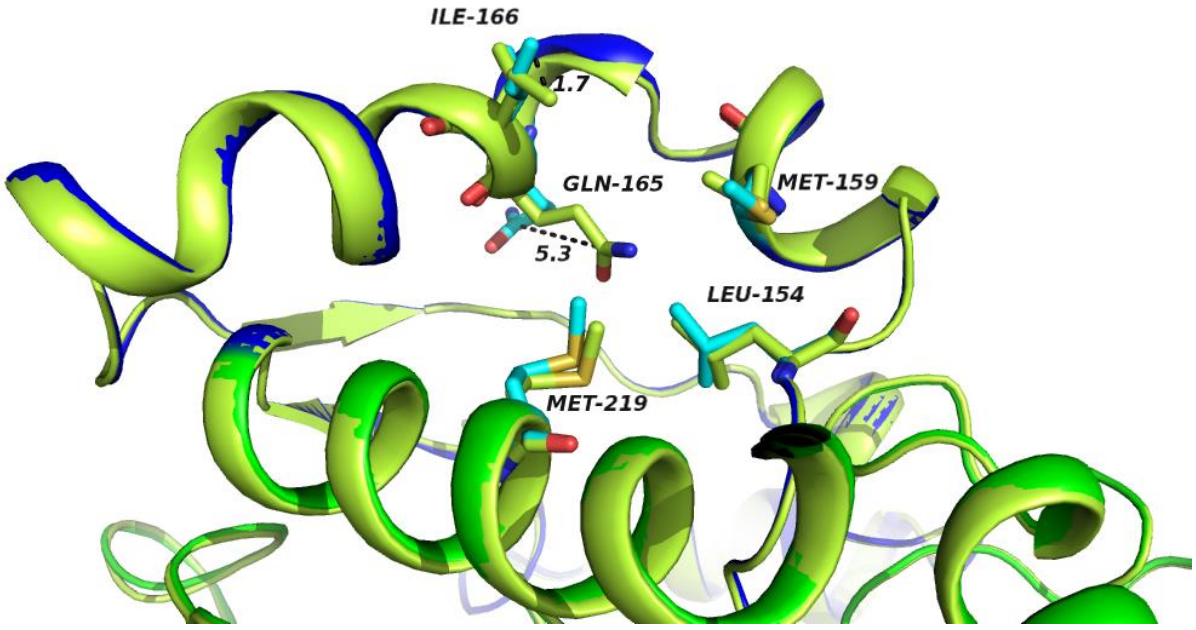

Figure 38 Superposition of the open free form of YJU3p (Chain D, green sidechains) and the inhibitor bound form (Chain C, blue sidechains, substrate analogue not shown).

is also a second shift in ILE166 which is assumed to take the role of a hinge in analogy to I145 in bMGL (*31*).

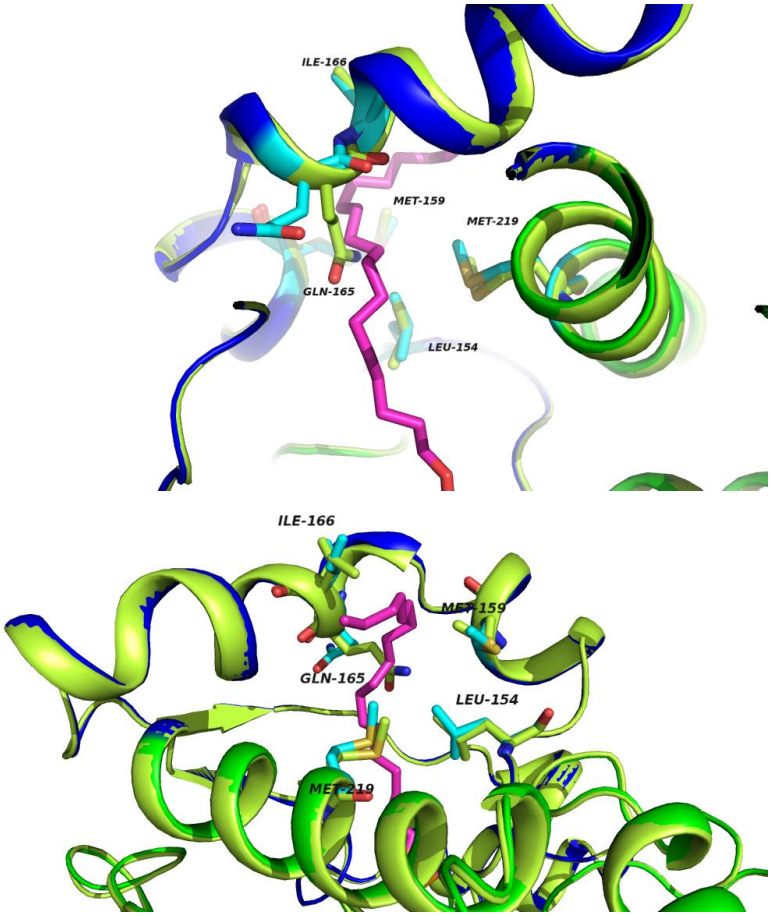

Figure 39 Superposition of the open free form of YJU3p (Chain D, green sidechains) and the inhibitor bound form (Chain C, blue sidechains). Inhibitor in Magenta

A superposition of the closed free form s-YJU3p, the open free form of s-YJU3p and the open substrate analogue bound form of s-YJU3p shows that the high flexibility of GLN165 is needed for the substrate to fit. The backbone shift leads to a 3.2Å shift of the C_δ of GLN165 therefore enabling the sidechain to be pushed out further by the substrate analogue. Overall the C_δ of the GLN165 sidechain is moved for 4.4Å which seem to be made up from two movements, the backbone changes and the movement of the sidechain itself, the second of which can probably be attributed to a "push" by the carbon tail, this could also be the sign of a larger movement, or a more open form of the cap region (Figure 40). These two movements which seem to be in different directions make up for the overall movement of the C_δ of 4.4Å which is sufficient to fit

a carbon chain through this “hole” with the Van der Waals radius of a CH3 group being around 2Å.

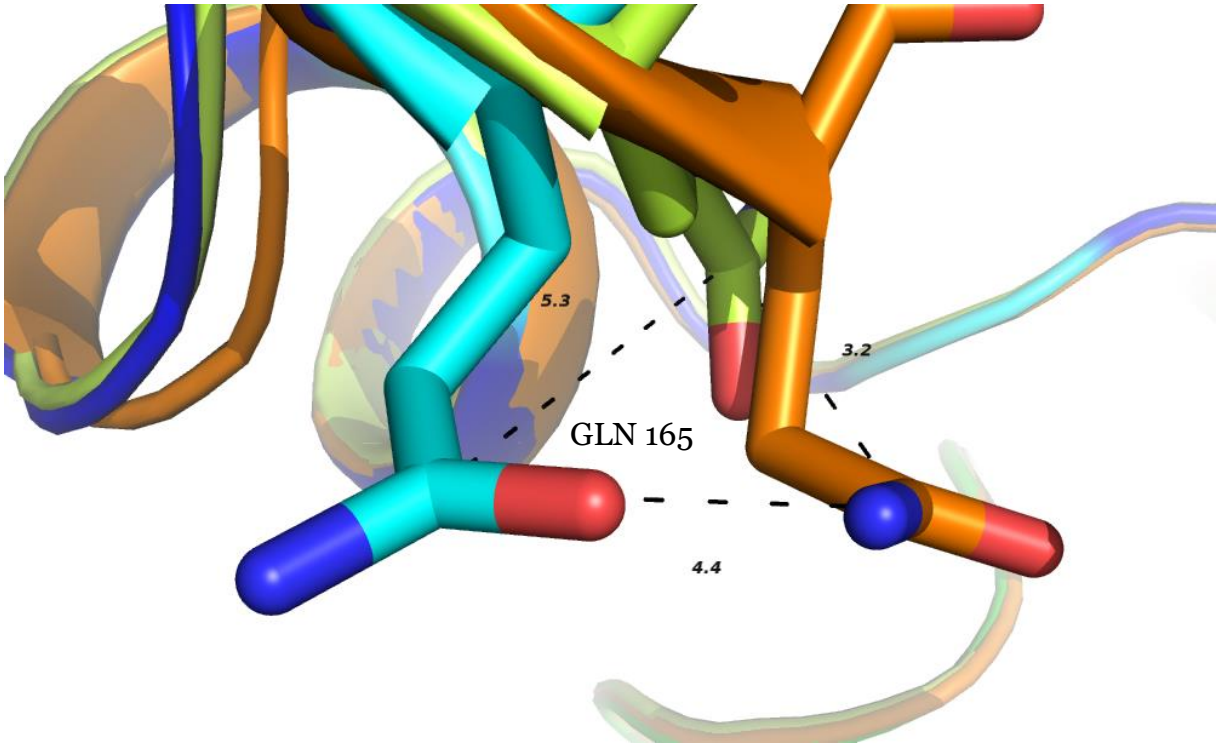

Figure 40 Superposition of the closed free form s-YJU3p (Chain A, orange), the open free form of s-YJU3p (Chain D, green) and the open substrate analogue bound form of s-YJU3p (Chain C, blue)

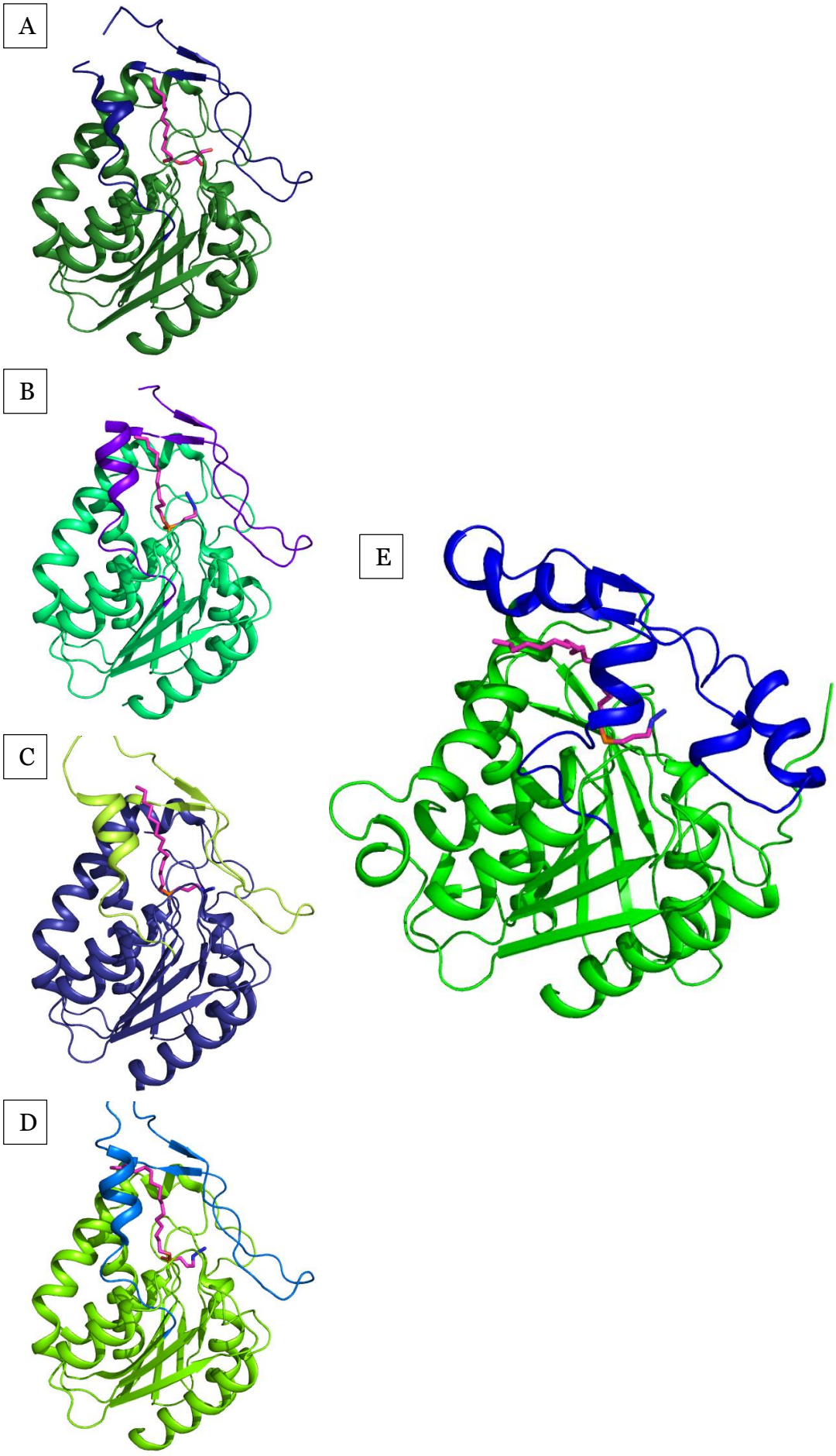

Figure 41 Comparison of different bMGL- substrate analogue complexes (A=C12 (PDB 4KE6), B=C14 (PDB 4KE7), C=C16PDB (4KE8) D=C18 (PDB= 4KE9) with E= YJU3-substrate analogue complex in cartoon representation

The second question that immediately comes to mind is if the structure and function of s-YJU3p and its C20 substrate analogue bound complex have similarities to already known structures of MGLs. The most important structures for this cause were provided by bMGL. The bMGL structure has already been determined in free form and bound to a large variety of substrate analogues and inhibitors, most importantly the C12 to C18 substrate analogues also used for my work on s-YJU3p. The only drawback in this situation was that bMGL has never been crystallized with the C20 substrate analogue which is the only substrate analog that yielded complex crystals with s-YJU3p. By studying the different structures of bMGL (Figure 41), at first from C12-C16, the thing that strikes is that there seem to be different release mechanisms for the carbon chain in s-YJU3p and bMGL. The carbon chain in bMGL sticks out through the cap, the carbon chain in s-YJU3p seems to be wedged between the first two α-helices of the cap and the first helix following the cap. But upon comparison of the bMGL C18 structure with the s-YJU3p C20 structure a certain degree of similarity in the cap region seems to be apparent (Figure 42,). In figure 42 it can be seen that in both cases (A: bMGL, B:s-YJU3p) the tail of the carbon chain is somewhat trapped between the first α-helix belonging to the cap region and the first α-helix already belonging to the α/β-hydrolase core. Upon further investigation it shows that the tails of the carbon chains of the substrate analogs are kept in place by non-polar interaction and that they are “pushing”

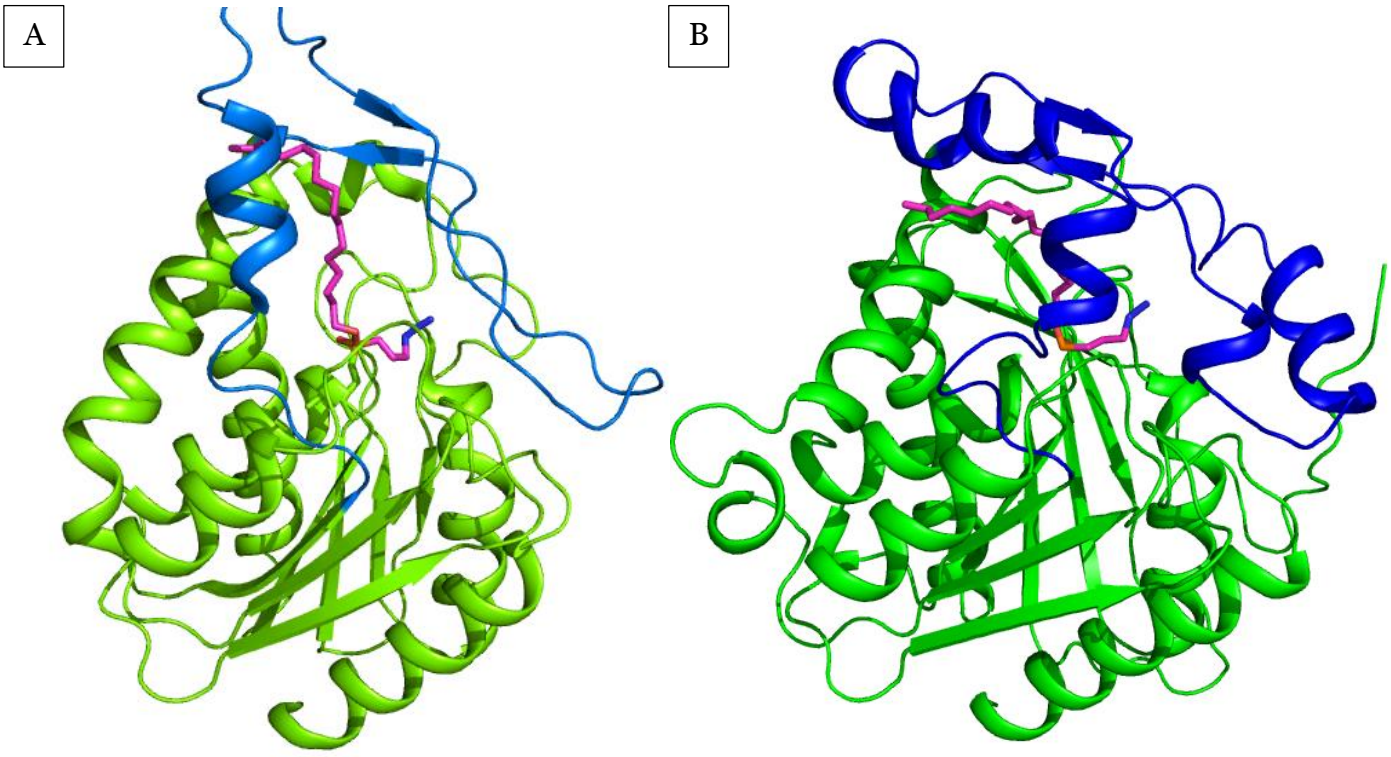

Figure 42 Comparison between bMGL-C18 complex (A) and s-YJU3p C20 complex (B) in cartoon representation

away polar sidechains like before mentioned GLN165 (Figure 40). In both cases the carbon chain is restricted from every direction (dotted lines are inserted between the atoms closest to each other between the substrate analogue and the sidechains (Figure 43). Further investigation of the cap region (Figure 43) shows that the alkyl chain is kept in place between the three α-helices in YJU3p and between two α-helices with the involvement of LEU138, which is located after the helix in the unstructured part of the bMGL cap and has a comparable position to ILE166 in YJU3p.

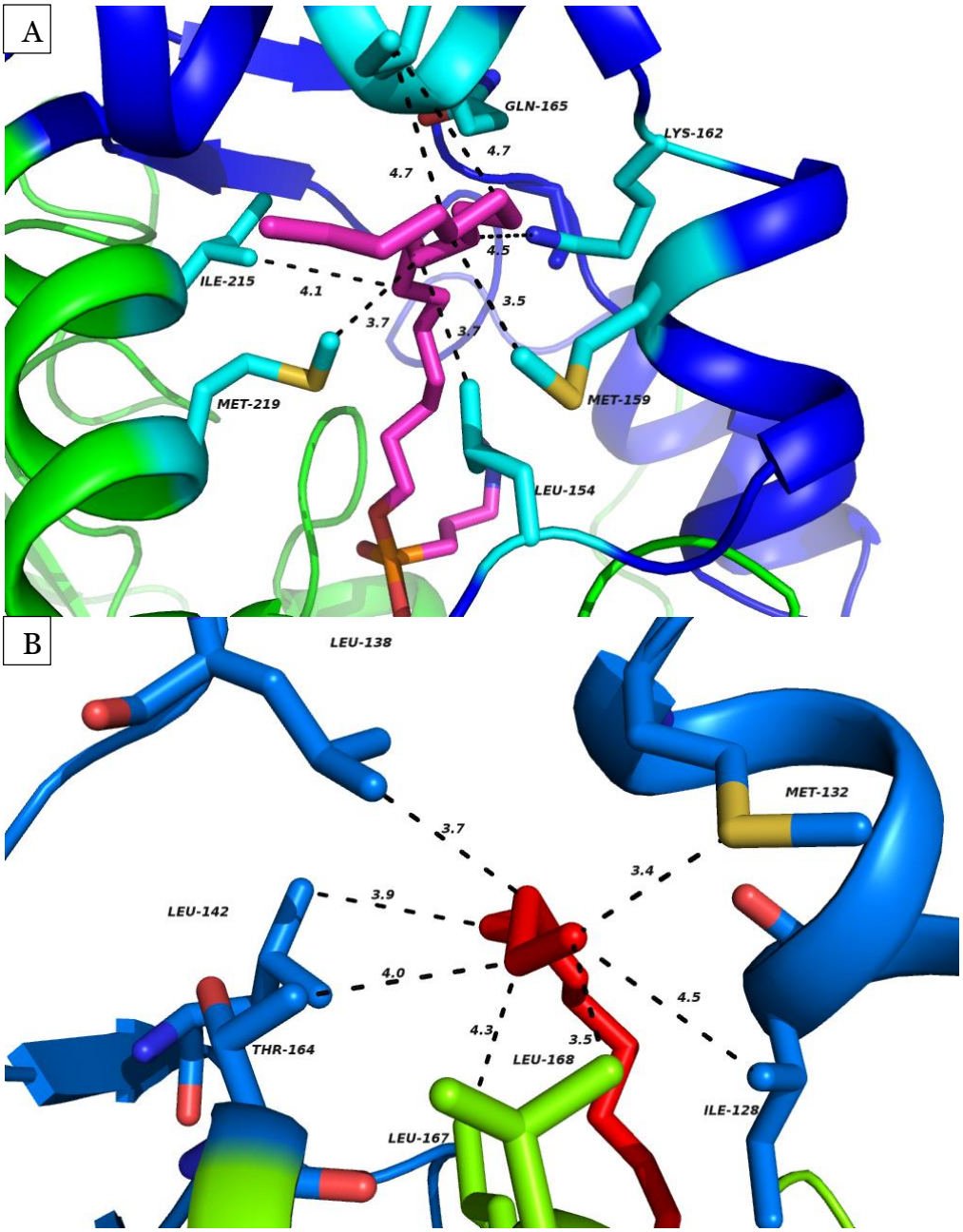

Figure 43 Distances between the closest sidechains and the substrate analogue bound forms of s-YJU3p (A) and bMGL (B)

In protein crystallography it's only possible to see snapshots of the movement of proteins. Therefore it is hard to say, with current information only, if the mechanisms of substrate capture and release are the same for bMGL and YJU3p. It is shown that bMGL has twice as high activity for 1-monolauroyl glycerol than for 1-monooleoylglycerol (*31*) which also lack an explanation at molecular detail. For YJU3p, only reaction rates for 1-monooleoylglycero have been shown in the literature (*33*) (Chapter2.4). More detailed activity assays with different substrates are currently ongoing in the laboratory of M. Oberer (unpublished data). According to Heier et al., and Rengachari et al., the reaction rates of YJU3p for 1-OG are about 30% higher than the reaction rates of bMGL but determining the reaction rate of YJU3p for shorter chain length monoglycerides could provide the next step in understanding the substrate release mechanism of monoglyceride lipases.

5. Collaborations

Prof. Dr. Rolf Breinbauer

Institute of Organic Chemistry

Graz University of Technology, Austria

E-Mail: breinbauer@tugraz.at

Ph.: +43/316/873 32400

Assoc. Prof. Dr. Ruth Birner-Grünberger

Institute for Pathology-Functional proteomics research group

Zentrum fuer medizinische Forschung (ZMF)- Massenspektrometrie/Proteomics Core Facility

Medical University of Graz, Austria

E-Mail: ruth.birner-gruenberger@medunigraz.at

Ph.:+43 (0)316 385-72962

6. References

1. Rengachari, S., Bezerra, G. A., Riegler-Berket, L., Gruber, C. C., Sturm, C., Taschler, U., Boeszoermenyi, A., Dreveny, I., Zimmermann, R., Gruber, K., and Oberer, M. The structure of monoacylglycerol lipase from Bacillus sp. H257 reveals unexpected conservation of the cap architecture between bacterial and human enzymes, *Biochim Biophys Acta 1821*, 1012-1021.
2. Fisch, F. (2009) The Link to X-Ray Protein Crystallography.
3. Kogoy. (2003) Protein Crystallization, Davidson College, Davidson.
4. Cockcroft, J. K. (1997-2006) Generation of X-rays, Birkbeck College, University of London, Birkbeck.
5. NIST. (2010) What is Synchrotron Radiation?, Nist, Gaithersburg.
6. Russo Krauss, I., Merlino, A., Vergara, A., and Sica, F. An overview of biological macromolecule crystallization, *International journal of molecular sciences 14*, 11643-11691.
7. Tornqvist, H., and Belfrage, P. (1976) Purification and some properties of a monoacylglycerol-hydrolyzing enzyme of rat adipose tissue, *J Biol Chem 251*, 813-819.
8. Fredrikson, G., Stralfors, P., Nilsson, N. O., and Belfrage, P. (1981) Hormone-sensitive lipase of rat adipose tissue. Purification and some properties, *J Biol Chem 256*, 6311-6320.
9. Zimmermann, R., Strauss, J. G., Haemmerle, G., Schoiswohl, G., Birner-Gruenberger, R., Riederer, M., Lass, A., Neuberger, G., Eisenhaber, F., Hermetter, A., and Zechner, R. (2004) Fat mobilization in adipose tissue is promoted by adipose triglyceride lipase, *Science 306*, 1383-1386.
10. Lowe, M. E. (2002) The triglyceride lipases of the pancreas, *J Lipid Res 43*, 2007-2016.
11. Watt, M. J., and Steinberg, G. R. (2008) Regulation and function of triacylglycerol lipases in cellular metabolism, *Biochem J 414*, 313-325.
12. Schalk-Hihi, C., Schubert, C., Alexander, R., Bayoumy, S., Clemente, J. C., Deckman, I., DesJarlais, R. L., Dzordzorme, K. C., Flores, C. M., Grasberger, B., Kranz, J. K., Lewandowski, F., Liu, L., Ma, H., Maguire, D., Macielag, M. J., McDonnell, M. E., Mezzasalma Haarlander, T., Miller, R., Milligan, C., Reynolds, C., and Kuo, L. C. Crystal structure of a soluble form of human monoglyceride lipase in complex with an inhibitor at 1.35 A resolution, *Protein Sci 20*, 670-683.
13. Muranushi, N., Takagi, N., Muranishi, S., and Sezaki, H. (1981) Effect of fatty acids and monoglycerides on permeability of lipid bilayer, *Chem Phys Lipids 28*, 269-279.
14. Bergsson, G., Steingrimsson, O., and Thormar, H. (2002) Bactericidal effects of fatty acids and monoglycerides on Helicobacter pylori, *Int J Antimicrob Agents 20*, 258-262.
15. Conley, A. J., and Kabara, J. J. (1973) Antimicrobial action of esters of polyhydric alcohols, *Antimicrob Agents Chemother 4*, 501-506.
16. Karlsson, M., Contreras, J. A., Hellman, U., Tornqvist, H., and Holm, C. (1997) cDNA cloning, tissue distribution, and identification of the catalytic triad of monoglyceride lipase. Evolutionary relationship to esterases, lysophospholipases, and haloperoxidases, *J Biol Chem 272*, 27218-27223.

17. Karlsson, M., Reue, K., Xia, Y. R., Lusis, A. J., Langin, D., Tornqvist, H., and Holm, C. (2001) Exon-intron organization and chromosomal localization of the mouse monoglyceride lipase gene, *Gene 272*, 11-18.
18. Karlsson, M., Tornqvist, H., and Holm, C. (2000) Expression, purification, and characterization of histidine-tagged mouse monoglyceride lipase from baculovirus-infected insect cells, *Protein Expr Purif 18*, 286-292.
19. Bertrand, T., Auge, F., Houtmann, J., Rak, A., Vallee, F., Mikol, V., Berne, P. F., Michot, N., Cheuret, D., Hoornaert, C., and Mathieu, M. Structural basis for human monoglyceride lipase inhibition, *J Mol Biol 396*, 663-673.
20. Cotes, K., Dhouib, R., Douchet, I., Chahinian, H., de Caro, A., Carriere, F., and Canaan, S. (2007) Characterization of an exported monoglyceride lipase from Mycobacterium tuberculosis possibly involved in the metabolism of host cell membrane lipids, *Biochem J 408*, 417-427.
21. Labar, G., Bauvois, C., Borel, F., Ferrer, J. L., Wouters, J., and Lambert, D. M. Crystal structure of the human monoacylglycerol lipase, a key actor in endocannabinoid signaling, *Chembiochem 11*, 218-227.
22. Dinh, T. P., Kathuria, S., and Piomelli, D. (2004) RNA interference suggests a primary role for monoacylglycerol lipase in the degradation of the endocannabinoid 2-arachidonoylglycerol, *Mol Pharmacol 66*, 1260-1264.
23. Ye, L., Zhang, B., Seviour, E. G., Tao, K. X., Liu, X. H., Ling, Y., Chen, J. Y., and Wang, G. B. Monoacylglycerol lipase (MAGL) knockdown inhibits tumor cells growth in colorectal cancer, *Cancer Lett 307*, 6-17.
24. Nomura, D. K., Long, J. Z., Niessen, S., Hoover, H. S., Ng, S. W., and Cravatt, B. F. Monoacylglycerol lipase regulates a fatty acid network that promotes cancer pathogenesis, *Cell 140*, 49-61.
25. Mead, J. R., Irvine, S. A., and Ramji, D. P. (2002) Lipoprotein lipase: structure, function, regulation, and role in disease, *J Mol Med (Berl) 80*, 753-769.
26. Kitaura, S., Suzuki, K., and Imamura, S. (2001) Monoacylglycerol lipase from moderately thermophilic Bacillus sp. strain H-257: molecular cloning, sequencing, and expression in Escherichia coli of the gene, *J Biochem 129*, 397-402.
27. Gold, A. M., and Fahrney, D. (1964) SULFONYL FLUORIDES AS INHIBITORS OF ESTERASES. II. FORMATION AND REACTIONS OF PHENYLMETHANESULFONYL ALPHA-CHYMOTRYPSIN, *Biochemistry 3*, 783-791.
28. Long, J. Z., Li, W., Booker, L., Burston, J. J., Kinsey, S. G., Schlosburg, J. E., Pavon, F. J., Serrano, A. M., Selley, D. E., Parsons, L. H., Lichtman, A. H., and Cravatt, B. F. (2009) Selective blockade of 2-arachidonoylglycerol hydrolysis produces cannabinoid behavioral effects, *Nature chemical biology 5*, 37-44.
29. Savinainen, J. R., Kansanen, E., Pantsar, T., Navia-Paldanius, D., Parkkari, T., Lehtonen, M., Laitinen, T., Nevalainen, T., Poso, A., Levonen, A.-L., and Laitinen, J. T. Robust Hydrolysis of Prostaglandin Glycerol Esters by Human Monoacylglycerol Lipase (MAGL), *Molecular Pharmacology 86*, 522-535.
30. Laitinen, T., Navia-Paldanius, D., Rytilahti, R., Marjamaa, J. J. T., KaÅ™Ã-zkovÃi, J., Parkkari, T., Pantsar, T., Poso, A., Laitinen, J. T., and Savinainen, J. R. Mutation of Cys242 of Human Monoacylglycerol Lipase Disrupts Balanced Hydrolysis of 1- and 2-Monoacylglycerols and Selectively Impairs Inhibitor Potency, *Molecular Pharmacology 85*, 510-519.
31. Rengachari, S., Aschauer, P., Schittmayer, M., Mayer, N., Gruber, K., Breinbauer, R., Birner-Gruenberger, R., Dreveny, I., and Oberer, M. Conformational plasticity and ligand binding of bacterial monoacylglycerol lipase, *J Biol Chem 288*, 31093-31104.

32. Athenstaedt, K., Zweytick, D., Jandrositz, A., Kohlwein, S. D., and Daum, G. (1999) Identification and characterization of major lipid particle proteins of the yeast Saccharomyces cerevisiae, *J Bacteriol 181*, 6441-6448.
33. Heier, C., Taschler, U., Rengachari, S., Oberer, M., Wolinski, H., Natter, K., Kohlwein, S. D., Leber, R., and Zimmermann, R. Identification of Yju3p as functional orthologue of mammalian monoglyceride lipase in the yeast Saccharomycescerevisiae, *Biochim Biophys Acta 1801*, 1063-1071.
34. Vagin, A. A., Steiner, R. A., Lebedev, A. A., Potterton, L., McNicholas, S., Long, F., and Murshudov, G. N. (2004) REFMAC5 dictionary: organization of prior chemical knowledge and guidelines for its use, *Acta Crystallogr D Biol Crystallogr 60*, 2184-2195.
35. Emsley, P., Lohkamp, B., Scott, W. G., and Cowtan, K. Features and development of Coot, *Acta Crystallogr D Biol Crystallogr 66*, 486-501.
36. Schrodinger, LLC. (2010) The PyMOL Molecular Graphics System, Version 1.4.1.
37. Inoue, H., Nojima, H., and Okayama, H. (1990) High efficiency transformation of Escherichia coli with plasmids, *Gene 96*, 23-28.
38. Lusty, C. (1999) A gentle vapor-diffusion technique for cross-linking of protein crystals for cryocrystallography, *Journal of Applied Crystallography 32*, 106-112.
39. Leslie, A. G. W. (1992) Recent changes to the MOSFLM package for processing film and image plate data., *Joint CCP4 + ESF-EAMCB News-letter on Protein Crystallography No. 26*.
40. Evans, P. (2006) Scaling and assessment of data quality, *Acta Crystallographica Section D 62*, 72-82.
41. Evans, P. AIMLESS (CCP4: Supported Program), http://www.mrc-lmb.cam.ac.uk, Cambridge.
42. Vagin, A., and Teplyakov, A. Molecular replacement with MOLREP, *Acta Crystallogr D Biol Crystallogr 66*, 22-25.
43. Vagin, A., and Teplyakov, A. (1997) MOLREP: an Automated Program for Molecular Replacement, *Journal of Applied Crystallography 30*, 1022-1025.
44. Aschauer, P. (2013) Structural Investigation of Substrate Binding in Monoglyceride Lipases in *Institute of Molecular Biosciences* p76, Tu Graz, Graz.

7. Supplemental

7.1. HSQC NMR

Both bMGL WT and bMGL_I145G were freshly expressed in M9 minimal media containing 15N-NH_4Cl, and purified by Ni-affinity chromatography as described earlier. The purified protein was further subjected to Gel Filtration Chromatography and the monomeric fraction was concentrated to ~0.5 mM. 10% DMSO was added to the concentrated sample and 1H-15N HSQC of both wild type as well as I145G variants were recorded. The HSQCs could be overlaid to the previously assigned HSQC spectra (courtesy: Lina Reigler Berket). The assignments were copied and the shifted peaks were mapped back to the bMGL structure. It was observed that the shifted residues belong to the cap region of the protein and this demonstrates the crucial role of I145 in cap confirmation. (Protocol provided by Krishna Mohan Padmanabha Das)

7.1. Protein and DNA sequences

7.1.1. YJU3 L175S Q264R DNA sequence

Sequence from forward sequencing, the nucleotides coding the last 8 amino acids cannot be seen.

```
   1  ATGTCGTACT ACCATCACCA TCACCATCAC GATTACGATA TCCCAACGAC CGAAAACCTG
  61  TATTTTCAGG GCGCCATGGG ATCCGCTCCG TATCCATACA AAGTGCAGAC GACAGTACCT
 121  GAACTTCAAT ACGAAAACTT TGATGGTGCT AAGTTCGGGT ACATGTTCTG GCCTGTTCAA
 181  AATGGCACCA ATGAGGTCAG AGGTAGAGTT TTACTGATTC ATGGGTTTGG CGAGTACACA
 241  AAGATTCAAT TCCGGCTTAT GGACCACTTA TCACTCAATG GTTACGAGTC ATTTACGTTT
 301  GATCAAAGGG GTGCTGGTGT TACATCGCCG GGCAGATCGA AAGGTGTAAC TGATGAGTAC
 361  CATGTGTTTA ACGATCTTGA GCATTTTGTG GAGAAGAACT TGAGTGAATG TAAGGCCAAA
 421  GGCATACCCT TGTTCATGTG GGGGCATTCA ATGGGCGGTG GTATCTGCCT AAACTATGCC
 481  TGCCAAGGTA AGCACAAAAA CGAAATAAGC GGATATATCG GGTCAGGCCC ATTAATAATT
 541  TTACATCCGC ATACAATGTA TAACAAGCCG ACCCAAATTA TTGCTCCATT ATTGGCGAAA
 601  TTTTCACCAA GGGTAAGGAT CGACACTGGT TTAGATCTTA AAGGAATCAC ATCTGATAAA
 661  GCCTATCGTG CTTTCCTCGG AAGCGATCCT ATGTCTGTTC CACTATATGG GTCGTTTAGG
 721  CAAATACACG ACTTTATGCA ACGTGGTGCC AAGCTCTACA AGAATGAAAA CAATTATATT
 781  CAGAAGAACT TCGCTAAAGA CAAACCCGTT ATTATTATGC ATGGACAAGA CGACACAATC
 841  AACGATCCTA AGGGCTCTGA AAAGTTCATT CGGGACTGTC CTTCTGCTGA CAAAGAATTA
 901  AAGCTGTATC CGGGCGCAAG ACATTCGATT TTCTCACTAG AGACAGATAA AGTCTTCAAC
 961  ACGGTGTTCA ATGATATGAA GCAATGGTTG GACAACCC
```

Linker and HIS tag
Start Codon
TTA to TCA
CAG to CGG

7.1.2. YJU3p WT and YJU3p L175S Q264R Protein Sequences

Protein sequence of s-YJU3p translated from sequence above. The nucleotides coding the last 8 amino acids cannot be seen in the sequencing.

```
CLUSTAL O(1.2.1) multiple sequence alignment

YJU3p       ---------------------------MAPYPYKVQTTVPELQYENFDGAKFGYMFWPVQ   33
s-YJU3p     MSYYHHHHHHDYDIPTTENLYFQGAMGSAPYPYKVQTTVPELQYENFDGAKFGYMFWPVQ   60
                                        ********************************

YJU3p       NGTNEVRGRVLLIHGFGEYTKIQFRLMDHLSLNGYESFTFDQRGAGVTSPGRSKGVTDEY   93
s-YJU3p     NGTNEVRGRVLLIHGFGEYTKIQFRLMDHLSLNGYESFTFDQRGAGVTSPGRSKGVTDEY   120
            ************************************************************

YJU3p       HVFNDLEHFVEKNLSECKAKGIPLFMWGHSMGGGICLNYACQGKHKNEISGYIGSGPLII   153
s-YJU3p     HVFNDLEHFVEKNLSECKAKGIPLFMWGHSMGGGICLNYACQGKHKNEISGYIGSGPLII   180
            ************************************************************

YJU3p       LHPHTMYNKPTQIIAPLLAKFLPRVRIDTGLDLKGITSDKAYRAFLGSDPMSVPLYGSFR   213
s-YJU3p     LHPHTMYNKPTQIIAPLLAKFSPRVRIDTGLDLKGITSDKAYRAFLGSDPMSVPLYGSFR   240
            ******************** ***************************************

YJU3p       QIHDFMQRGAKLYKNENNYIQKNFAKDKPVVIMHGQDDTINDPKGSEKFIQDCPSADKEL   273
s-YJU3p     QIHDFMQRGAKLYKNENNYIQKNFAKDKPVIIMHGQDDTINDPKGSEKFIRDCPSADKEL   300
            ****************************:******************:*********

YJU3p       KLYPGARHSIFSLETDEVFNTVFNDMKQWLDKHTTTEAKP    313
s-YJU3p     KLYPGARHSIFSLETDKVFNTVFNDMKQWLDN--------    332
            ***************:**************:
```

7.1.3. bMGL Wildtype and bMG LI145G Mutant Sequence Alignment

Sequences provided by Philipp Aschauer (*44*)

```
bMGL-originalgene      ------------------------------ATGGGCAGCAGCCATCATCATCATCATCA 29
pET28a-bMGLI145G       ATTTTGTTTAACTTTAAGAAGGAGATATACCATGGGCAGCAGCCATCATCATCATCATCA 60
                                                     ******************************

bMGL-originalgene      CAGCAGCGGCCTGGTGCCGCGCGGCAGCCATATGAGCGAACAATATCCGGTGCTCTCGGG 89
pET28a-bMGLI145G       CAGCAGCGGCCTGGTGCCGCGCGGCAGCCATATGAGCGAACAATATCCGGTGCTCTCGGG 120
                       ************************************************************

bMGL-originalgene      CGCCGAGCCGTTTTACGCCGAAAACGGGCCGGTCGGGGTGCTGCTCGTGCACGGATTCAC 149
pET28a-bMGLI145G       CGCCGAGCCGTTTTACGCCGAAAACGGGCCGGTCGGGGTGCTGCTCGTGCACGGATTCAC 180
                       ************************************************************

bMGL-originalgene      CGGCACGCCCCACAGCATGCGCCCGCTCGCTGAAGCGTATGCGAAAGCCGGCTATACCGT 209
pET28a-bMGLI145G       CGGCACGCCCCACAGCATGCGCCCGCTCGCTGAAGCGTATGCGAAAGCCGGCTATACCGT 240
                       ************************************************************

bMGL-originalgene      TTGCCTGCCGCGCTTAAAAGGGCACGGAACGCATTACGAAGACATGGAACGGACGACGTT 269
pET28a-bMGLI145G       TTGCCTGCCGCGCTTAAAAGGGCACGGAACGCATTACGAAGACATGGAACGGACGACGTT 300
                       ************************************************************

bMGL-originalgene      CCACGATTGGGTCGCCTCGGTCGAAGAAGGATATGGATGGCTGAAACAACGATGCCAAAC 329
pET28a-bMGLI145G       CCACGATTGGGTCGCCTCGGTCGAAGAAGGATATGGATGGCTGAAACAACGATGCCAAAC 360
                       ************************************************************

bMGL-originalgene      CATTTTTGTCACCGGGCTGTCGATGGGCGGGACGCTCACGCTTTATTTGGCGGAACATCA 389
pET28a-bMGLI145G       CATTTTTGTCACCGGGCTGTCGATGGGCGGGACGCTCACGCTTTATTTGGCGGAACATCA 420
                       ************************************************************

bMGL-originalgene      CCCAGACATCTGCGGCATCGTGCCGATTAACGCCGCTGTCGACATCCCGGCCATCGCCGC 449
pET28a-bMGLI145G       CCCAGACATCTGCGGCATCGTGCCGATTAACGCCGCTGTCGACATCCCGGCCATCGCCGC 480
                       ************************************************************

bMGL-originalgene      CGGGATGACGGGCGGGGGCGAGCTGCCGAGGTATCTGGATTCGATCGGTTCGGACTTGAA 509
pET28a-bMGLI145G       CGGGATGACGGGCGGGGGCGAGCTGCCGAGGTATCTGGATTCGGGCGGTTCGGACTTGAA 540
                       ******************************************. ***************

bMGL-originalgene      AAATCCGGATGTGAAAGAGCTGGCATACGAGAAAACGCCGACCGCTTCGCTTCTTCAGCT 569
pET28a-bMGLI145G       AAATCCGGATGTGAAAGAGCTGGCATACGAGAAAACGCCGACCGCTTCGCTTCTTCAGCT 600
                       ************************************************************

bMGL-originalgene      GGCTAGGCTGATGGCACAGACAAAAGCGAAACTCGATCGCATCGTCTGTCCGGCGTTGAT 629
pET28a-bMGLI145G       GGCTAGGCTGATGGCACAGACAAAAGCGAAACTCGATCGCATCGTCTGTCCGGCGTTGAT 660
                       ************************************************************

bMGL-originalgene      TTTTGTCTCCGACGAAGATCACGTCGTGCCGCCGGGAAACGCCGACATCATCTTTCAAGG 689
pET28a-bMGLI145G       TTTTGTCTCCGACGAAGATCACGTCGTGCCGCCGGGAAACGCCGACATCATCTTTCAAGG 720
                       ************************************************************

bMGL-originalgene      CATTTCATCGACGGAGAAAGAGATCGTCCGCCTCCGAAACAGCTACCATGTGGCGACGCT 749
pET28a-bMGLI145G       CATTTCATCGACGGAGAAAGAGATCGTCCGCCTCCGAAACAGCTACCATGTGGCGACGCT 780
                       ************************************************************

bMGL-originalgene      CGATTACGACCAACCGATGATTATTGAACGGTCTCTCGAATTTTTCGCCAAGCACGCCGG 809
pET28a-bMGLI145G       CGATTACGACCAACCGATGATTATTGAACGGTCTCTCGAATTTTTCGCCAAGCACGCCGG 840
                       ************************************************************

bMGL-originalgene      ATAACTCGAG---------------------------------------------------- 813
pET28a-bMGLI145G       ATAACTCGAGCACCACCACCACCACCACTGAGATCCGGCTGCTAACAAAGCCCGAAAGGA 900
                       **********
```

Histag sequence and linker region

NdeI site-CATATG; XhoI site-CTCGAG

Stop codon-TAA

Mutation: ATC to GGC

7.1.4. bMGL Wildtype and bMG LI145S Mutant Sequence Alignment

Sequences provided by Philipp Aschauer (*44*)

```
bMGL-originalgene      ----------------------------ATGGGCAGCAGCCATCATCATCATCACA 31
pET28a-bMGLI145S       TTTGTTTAACTTTAAGAAGGAGATATACCATGGGCAGCAGCCATCATCATCATCACA 60
                                                   ****************************

bMGL-originalgene      GCAGCGGCCTGGTGCCGCGCGGCAGCCATATGAGCGAACAATATCCGGTGCTCTCGGGCG 91
pET28a-bMGLI145S       GCAGCGGCCTGGTGCCGCGCGGCAGCCATATGAGCGAACAATATCCGGTGCTCTCGGGCG 120
                       ************************************************************

bMGL-originalgene      CCGAGCCGTTTTACGCCGAAAACGGGCCGGTCGGGGTGCTGCTCGTGCACGGATTCACCG 151
pET28a-bMGLI145S       CCGAGCCGTTTTACGCCGAAAACGGGCCGGTCGGGGTGCTGCTCGTGCACGGATTCACCG 180
                       ************************************************************

bMGL-originalgene      GCACGCCCCACAGCATGCGCCCGCTCGCTGAAGCGTATGCGAAAGCCGGCTATACCGTTT 211
pET28a-bMGLI145S       GCACGCCCCACAGCATGCGCCCGCTCGCTGAAGCGTATGCGAAAGCCGGCTATACCGTTT 240
                       ************************************************************

bMGL-originalgene      GCCTGCCGCGCTTAAAAGGGCACGGAACGCATTACGAAGACATGGAACGGACGACGTTCC 271
pET28a-bMGLI145S       GCCTGCCGCGCTTAAAAGGGCACGGAACGCATTACGAAGACATGGAACGGACGACGTTCC 300
                       ************************************************************

bMGL-originalgene      ACGATTGGGTCGCCTCGGTCGAAGAAGGATATGGATGGCTGAAACAACGATGCCAAACCA 331
pET28a-bMGLI145S       ACGATTGGGTCGCCTCGGTCGAAGAAGGATATGGATGGCTGAAACAACGATGCCAAACCA 360
                       ************************************************************

bMGL-originalgene      TTTTTGTCACCGGGCTGTCGATGGGCGGGACGCTCACGCTTTATTTGGCGGAACATCACC 391
pET28a-bMGLI145S       TTTTTGTCACCGGGCTGTCGATGGGCGGGACGCTCACGCTTTATTTGGCGGAACATCACC 420
                       ************************************************************

bMGL-originalgene      CAGACATCTGCGGCATCGTGCCGATTAACGCCGCTGTCGACATCCCGGCCATCGCCGCCG 451
pET28a-bMGLI145S       CAGACATCTGCGGCATCGTGCCGATTAACGCCGCTGTCGACATCCCGGCCATCGCCGCCG 480
                       ************************************************************

bMGL-originalgene      GGATGACGGGCGGGGGCGAGCTGCCGAGGTATCTGGATTCGATCGGTTCGGACTTGAAAA 511
pET28a-bMGLI145S       GGATGACGGGCGGGGGCGAGCTGCCGAGGTATCTGGATTCGAGCGGTTCGGACTTGAAAA 540
                       ****************************************** ****************

bMGL-originalgene      ATCCGGATGTGAAAGAGCTGGCATACGAGAAAACGCCGACCGCTTCGCTTCTTCAGCTGG 571
pET28a-bMGLI145S       ATCCGGATGTGAAAGAGCTGGCATACGAGAAAACGCCGACCGCTTCGCTTCTTCAGCTGG 600
                       ************************************************************

bMGL-originalgene      CTAGGCTGATGGCACAGACAAAAGCGAAACTCGATCGCATCGTCTGTCCGGCGTTGATTT 631
pET28a-bMGLI145S       CTAGGCTGATGGCACAGACAAAAGCGAAACTCGATCGCATCGTCTGTCCGGCGTTGATTT 660
                       ************************************************************

bMGL-originalgene      TTGTCTCCGACGAAGATCACGTCGTGCCGCCGGGAAACGCCGACATCATCTTTCAAGGCA 691
pET28a-bMGLI145S       TTGTCTCCGACGAAGATCACGTCGTGCCGCCGGGAAACGCCGACATCATCTTTCAAGGCA 720
                       ************************************************************

bMGL-originalgene      TTTCATCGACGGAGAAAGAGATCGTCCGCCTCCGAAACAGCTACCATGTGGCGACGCTCG 751
pET28a-bMGLI145S       TTTCATCGACGGAGAAAGAGATCGTCCGCCTCCGAAACAGCTACCATGTGGCGACGCTCG 780
                       ************************************************************

bMGL-originalgene      ATTACGACCAACCGATGATTATTGAACGGTCTCTCGAATTTTTCGCCAAGCACGCCGGAT 811
pET28a-bMGLI145S       ATTACGACCAACCGATGATTATTGAACGGTCTCTCGAATTTTTCGCCAAGCACGCCGGAT 840
                       ************************************************************

bMGL-originalgene      AACTCGAG-------------------------------------------------- 813
pET28a-bMGLI145S       AACTCGAGCACCACCACCACCACCACTGAGATCCGGCTGCTAACAAAGCCCGAAAGGAAGC  900
                       ********
```

Histag sequence and linker region

NdeI site-CATATG; XhoI site-CTCGAG

Stop codon-TAA

Mutation: ATC to AGC

7.1.5. Multiple MGLs Sequence Alignments

Protein sequence of YJU3p-L175S-Q264R (s-YJU3p) translated from sequence above. The nucleotides coding the last 8 amino acids cannot be seen in the sequencing.

```
bMGL                  --------------MSEQYPVL---SGAEPFYA-------ENGP-VGVLLVHGFTGTPHS
bMGL-I145G            --------------MSEQYPVL---SGAEPFYA-------ENGP-VGVLLVHGFTGTPHS
bMGL-I145S            --------------MSEQYPVL---SGAEPFYA-------ENGP-VGVLLVHGFTGTPHS
YJU3p-L175S-Q264R     MGSAPYPYKVQTTVPELQYE---NFDGAKFGYMFWPVQNGTNEVRGRVLLIHGFGEYTKI
hMGL                  MPEESSPRRTPQSIPYQDLPHLVNADGQYLFCRYWKP---TGTPKALIFVSHGAGEHSGR
                                       :       .*                    ::: **

bMGL                  MRPLAEAYAKAGYTVCLPRLKGHGTHYEDME---RTTFHDWVA---SVEEGYGWLKQRCQ
bMGL-I145G            MRPLAEAYAKAGYTVCLPRLKGHGTHYEDME---RTTFHDWVA---SVEEGYGWLKQRCQ
bMGL-I145S            MRPLAEAYAKAGYTVCLPRLKGHGTHYEDME---RTTFHDWVA---SVEEGYGWLKQRCQ
YJU3p-L175S-Q264R     QFRLMDHLSLNGYESFTFDQRGAGVTSPGRSKGVTDEYHVFNDLEHFVEKNLSECKAKGI
hMGL                  YEELARM--LMGLDLLVFAHDHVGHGQSEGERMVVSDFHVFVRDV-LQHVDSMQKDYPGL
                         *       *           *      .      :* :       .      .

bMGL                  TIFVTGLSMGGTLTLYLAEHH---PDICGIVPINAAVDI--------PA-IAAGMTGGGE
bMGL-I145G            TIFVTGLSMGGTLTLYLAEHH---PDICGIVPINAAVDG--------PA-IAAGMTGGGE
bMGL-I145S            TIFVTGLSMGGTLTLYLAEHH---PDICGIVPINAAVDS--------PA-IAAGMTGGGE
YJU3p-L175S-Q264R     PLFMWGHSMGGGICLNYACQGKHKNEISGYIGSGPLIILHPHTMYNKPTQIIAPL-LAKF
hMGL                  PVFLLGHSMGGAIAILTAAER--PGHFAGMVLISPLVLANPESATTFKV-LAAKV-LNLV
                       :*: * **** : :  * .     .:.* :     :           . : * :

bMGL                  LPRYLDSIGSDLKN--PDVKEL-AYEKTPTA-----SLLQ----------LARLMAQTKA
bMGL-I145G            LPRYLDSIGSDLKN--PDVKEL-AYEKTPTA-----SLLQ----------LARLMAQTKA
bMGL-I145S            LPRYLDSIGSDLKN--PDVKEL-AYEKTPTA-----SLLQ----------LARLMAQTKA
YJU3p-L175S-Q264R     SPRVRIDTGLDLKGITSDKAYRAFLGSDPMSVPLYGSFRQIHDFMQRGAKLYKNENNYIQ
hMGL                  LPNLSLG-PIDSSVLSRNKTEVDIYNSDPLICRAG--LK-----VCFGIQLLNAVSRVER
                       *.       * .    :        . *        :            * .   .

bMGL                  KLDRIVCPALIFVSDEDHVVPPGNADIIFQGISSTEKEIVRLRNSYHVATL-DYDQP--M
bMGL-I145G            KLDRIVCPALIFVSDEDHVVPPGNADIIFQGISSTEKEIVRLRNSYHVATL-DYDQP--M
bMGL-I145S            KLDRIVCPALIFVSDEDHVVPPGNADIIFQGISSTEKEIVRLRNSYHVATL-DYDQP--M
YJU3p-L175S-Q264R     KNFAKDKPVIIMHGQDDTINDPKGSEKFIRDCPSADKELKLYPGARHSIFSLETDKVFNT
hMGL                  ALPKLTVPFLLLQGSADRLCDSKGAYLLMELAKSQDKTLKIYEGAYHVLH-KELPEVTNS
                             * ::: .. * :     :  ::.   * :* :     : *     :  :

bMGL                  IIERSLEFFAK---HAG--
bMGL-I145G            IIERSLEFFAK---HAG--
bMGL-I145S            IIERSLEFFAK---HAG--
YJU3p-L175S-Q264R     VFNDMKQWLDN--------
hMGL                  VFHEINMWVSQRTATAGTA
                      ::.    :. :

CLUSTAL O(1.2.1) multiple sequence alignment
```